Title

The long noncoding RNA ROCKI regulates inflammatory gene expression.

Journal

The EMBO journal, 38(8)

ISSN

0261-4189

Authors

Zhang, Qiong
Chao, Ti-Chun
Patil, Veena S
et al.

Publication Date

2019-04-01

DOI

10.15252/embj.2018100041

Peer reviewed

Article

SOURCE DATA | OPEN ACCESS

THE EMBO JOURNAL

The long noncoding RNA *ROCKI* regulates inflammatory gene expression

Qiong Zhang[1,¶], Ti-Chun Chao[1,¶], Veena S Patil[1,†,¶], Yue Qin[1], Shashi Kant Tiwari[1], Joshua Chiou[1], Alexander Dobin[2], Chih-Ming Tsai[1,‡], Zhonghan Li[1,§], Jason Dang[1], Shagun Gupta[1], Kevin Urdahl[3,4], Victor Nizet[1,5], Thomas R Gingeras[2], Kyle J Gaulton[1] & Tariq M Rana[1,*]

Abstract

Long noncoding RNAs (lncRNAs) can regulate target gene expression by acting in *cis* (locally) or in *trans* (non-locally). Here, we performed genome-wide expression analysis of Toll-like receptor (TLR)-stimulated human macrophages to identify pairs of *cis*-acting lncRNAs and protein-coding genes involved in innate immunity. A total of 229 gene pairs were identified, many of which were commonly regulated by signaling through multiple TLRs and were involved in the cytokine responses to infection by group B *Streptococcus*. We focused on elucidating the function of one lncRNA, named *lnc-MARCKS* or *ROCKI* (Regulator of Cytokines and Inflammation), which was induced by multiple TLR stimuli and acted as a master regulator of inflammatory responses. *ROCKI* interacted with APEX1 (apurinic/apyrimidinic endodeoxyribonuclease 1) to form a ribonucleoprotein complex at the *MARCKS* promoter. In turn, *ROCKI*–APEX1 recruited the histone deacetylase HDAC1, which removed the H3K27ac modification from the promoter, thus reducing *MARCKS* transcription and subsequent Ca^{2+} signaling and inflammatory gene expression. Finally, genetic variants affecting *ROCKI* expression were linked to a reduced risk of certain inflammatory and infectious disease in humans, including inflammatory bowel disease and tuberculosis. Collectively, these data highlight the importance of *cis*-acting lncRNAs in TLR signaling, innate immunity, and pathophysiological inflammation.

Keywords cytokine production; host–pathogen interactions; innate immune system; lncRNA; TLRs

Subject Categories Immunology; Microbiology, Virology & Host Pathogen Interaction; RNA Biology

DOI 10.15252/embj.2018100041 | Received 13 June 2018 | Revised 12 February 2019 | Accepted 14 February 2019 | Published online 27 March 2019

The EMBO Journal (2019) 38: e100041

Introduction

To date, approximately 16,000 human and 12,000 mouse genes for long noncoding RNAs (lncRNAs; defined as > 200 nucleotides) have been identified, making them the largest known class of noncoding RNAs in the mammalian genome GENCODE (https://www.gencodegenes.org). lncRNAs are versatile regulators of gene expression that interact with DNA, RNA, and proteins, and function through multiple diverse mechanisms that include acting as scaffolds, decoys, and recruiters of genetic modifiers (Cech & Steitz, 2014; Quinn & Chang, 2016; Kopp & Mendell, 2018). Of particular interest, although lncRNAs are able to regulate the expression of neighboring genes (acting in *cis*) and/in distantly located genes (in *trans*), increasing evidence suggests that the majority act in *cis* (Guil & Esteller, 2012). Functional classification of lncRNAs is important for developing experimental approaches to understand lncRNA functions (Kopp & Mendell, 2018).

Innate immunity is a fundamental component of anti-pathogen defense in eukaryotes and is mediated by several families of cell surface and intracellular pattern recognition receptors, including Toll-like receptors (TLRs), C-type lectin receptors, RIG-I-like receptors, NOD-like receptors, and AIM2-like receptors (Mogensen, 2009). The innate immune system acts as a sensor of microbial infections to rapidly activate defense responses and to initiate long-lasting adaptive immunity (Iwasaki & Medzhitov, 2015). The human genome encodes about 10 TLR genes, each specialized in recognizing highly conserved structural motifs produced by microbial pathogens (pathogen-associated microbial patterns, PAMPs) (Song & Lee, 2012). TLRs can function as homodimers or heterodimers; for example, TLR2/TLR1 and TLR2/TLR6 heterodimers recognize lipopeptides from bacteria and mycoplasma; TLR4 and TLR5 homodimers recognize lipopolysaccharides (LPS) from Gram-negative bacteria and flagellin in

1 Department of Pediatrics, University of California San Diego School of Medicine, La Jolla, CA, USA
2 Cold Spring Harbor Laboratory, Cold Spring Harbor, NY, USA
3 Center for Infectious Disease Research (CIDR), Seattle, WA, USA
4 Department of Immunology, University of Washington School of Medicine, Seattle, WA, USA
5 Skaggs School of Pharmacy and Pharmaceutical Sciences, University of California San Diego School of Medicine, La Jolla, CA, USA
*Corresponding author. Tel: +858 246 1100; E-mail: trana@ucsd.edu
¶ These authors contributed equally to this work
† Present address: La Jolla Institute for Allergy and Immunology, La Jolla, CA, USA
‡ Present address: College of Life Science, Sichuan University, Chengdu, Sichuan, China
§ Present address: Division of Pediatric Infectious Diseases, Cedars-Sinai Medical Center (CSMC), Los Angeles, CA, USA

flagellate bacteria, respectively; and TLR3, 7, 8, and 9 homodimers respond to various forms of bacterial and viral nucleic acids (Gay & Gangloff, 2007). TLR stimulation initiates intracellular signaling cascades that lead to the production of anti-microbial genes such as the proinflammatory cytokines interleukin (IL)-1 and IL-6, tumor necrosis factor-α (TNF-α), and type I and II interferons (IFN-α/-β/-γ), which help orchestrate the innate anti-pathogen immune response (Kawai & Akira, 2010). These pro-inflammatory signaling networks are tightly regulated to ensure that cells mount a robust and timely response to pathogens while concomitantly guarding against excessive and sustained inflammation, which may promote the development of chronic inflammatory diseases.

Recent microarray and RNA sequencing data have shown that immune responses alter the expression of hundreds of lncRNAs (Carpenter *et al*, 2013; Rapicavoli *et al*, 2013; Li *et al*, 2014; Atianand *et al*, 2016; Wang *et al*, 2017), many of which are *trans*-acting regulators of protein-coding genes (Chen *et al*, 2017). For example, in TLR1/2-stimulated THP1-derived human macrophages, the lncRNA *THRIL* regulates TNF-α expression in *trans* by forming a complex with the ribonucleoprotein (RNP) hnRNPL that acts at the *TNF-α* promoter (Li *et al*, 2014). In another study, *lincRNA-COX2* was found to *trans*-regulate inflammatory gene expression in LPS-stimulated bone marrow-derived dendritic cells by interacting with hnRNP-A/B and hnRNP-A2/B1 (Carpenter *et al*, 2013). *NEAT1* is another *trans*-acting lncRNA that stimulates TLR3-stimulated IL-8 expression in HeLa cells by binding to the splicing factor SFPQ, thereby inducing SFPQ translocation away from the *IL-8* promoter (Imamura *et al*, 2014). While these studies confirm the importance of *trans* activity of lncRNAs in regulating innate immune responses, there remains a large gap in our understanding of the extent to which *cis*-regulatory lncRNAs contribute to physiological and pathogenic inflammatory responses.

Here, we sought to identify global changes in coding and noncoding gene expression during the innate immune response of macrophages to TLR ligands. We identified 229 differentially expressed lncRNAs located within 5 kb of protein-coding genes with immune-related functions, suggesting that they may be *cis*-regulatory lncRNAs with important roles in innate immunity. Consistent with this, three of the identified *cis*-acting lncRNA-coding gene pairs, *lnc-MARCKS*, *lnc-BCAT1*, and *lnc-BAIAP2*, were shown to regulate inflammatory gene expression in macrophages stimulated with a panel of TLR ligands or infected a leading human bacterial pathogen, group B *Streptococcus* (GBS). We investigated the function and regulatory mechanism of *lnc-MARCKS*, which we named Regulator of Cytokines and Inflammation (*ROCKI*), in more detail. We found that *ROCKI* regulated expression of its cognate protein-coding gene myristoylated alanine-rich protein kinase C (*MARCKS*) by forming an RNP complex at the *MARCKS* promoter with apurinic/apyrimidinic endodeoxyribonuclease 1 (APEX1). Notably, the APEX1–*ROCKI* complex induced recruitment of histone deacetylase HDAC1 to the promoter, which led to a reduction in the active enhancer mark H3K27ac and suppression of *MARCKS* transcription. In turn, *ROCKI*-mediated negative regulation of *MARCKS* promoted inflammatory cytokine and chemokine production. Finally, we identified genetic variants of *ROCKI* in human monocytes that are significantly associated with a reduced risk of inflammation-related (e.g., inflammatory bowel disease) and infection-related (e.g., *Mycobacterium tuberculosis*) disease phenotypes in humans.

Collectively, our findings advance our understanding of the mechanisms by which *cis*-acting lncRNAs regulate gene expression in response to bacterial and viral infections, and also suggest that *ROCKI*-regulated expression of *MARCKS* may contribute to inflammatory diseases.

Results

TLR signaling induces genome-wide changes in LncRNA- and protein-coding genes

To understand the global changes in protein-coding and noncoding gene expression induced by TLR activation, we analyzed the human THP1 monocyte cell line, which can be differentiated into macrophage-like cells by treatment with phorbol-12-myristate-13-acetate (PMA). These cells are commonly used to study TLR-mediated responses against bacterial and viral pathogens. To identify the optimal stimulation time, the cells were incubated for 2, 4, or 8 h with vehicle or one of three TLR ligands; Pam3CSK4 (Pam3), a bacterial triacyl lipoprotein mimetic and TLR1/2 ligand; Pam2CGDPKHPKSF (FSL-1), a synthetic diacyl lipoprotein from *Mycoplasma salivarium* and TLR2/6 ligand; or LPS from *Escherichia coli K12*, a TLR4 ligand. RT–qPCR analysis revealed that expression of the proinflammatory genes *IL8* and *IL12B* peaked at 8 h after stimulation (Fig EV1A–C). RNA-seq analysis also identified numerous differentially expressed protein-coding and lncRNA-coding genes in cells stimulated for 8 h by Pam3, FSL-1, or LPS compared with unstimulated cells (Fig 1A and B). The Circos plots in Fig 1 highlight changes in expression of two representative protein-coding genes (*NFκB*, *IFIT1*) (Lemaitre, 2004) and two lncRNA-coding genes (*NEAT1*, *Lnc-DC*) (Imamura *et al*, 2014; Wang *et al*, 2014), all of which are involved in host immune responses and are dynamically regulated in response to Pam3, LPS, and FSL-1 stimulation.

Identification of *Cis*-acting LncRNAs and protein-coding genes associated with TLR signaling

Although lncRNAs can regulate protein-coding gene expression by acting in *cis* or in *trans*, we focused here on identifying *cis*-regulatory lncRNAs in TLR-stimulated THP1-derived macrophages. We performed bioinformatics analysis of the differentially expressed paired lncRNA-coding and protein-coding genes in Pam3-, LPS-, and FSL-stimulated cells, and we selected all gene pairs located within 5 kb of each other (Fig 1C, Table EV1). Previous work has shown that most *cis*-acting lncRNA genes are located within 5 kb of their corresponding regulated protein-coding genes (Mondal *et al*, 2010; Orom *et al*, 2010; Cabili *et al*, 2011; Sigova *et al*, 2013; Luo *et al*, 2016).

Our analysis identified 229 candidate lncRNA-coding and protein-coding gene pairs, of which 116, 120, and 140 pairs were differentially expressed in cells stimulated with FSL-1, LPS, and Pam3, respectively, and 41 gene pairs were commonly regulated by all three TLRs (Fig 1E). Among the 229 lncRNAs, 203, 25, and 4

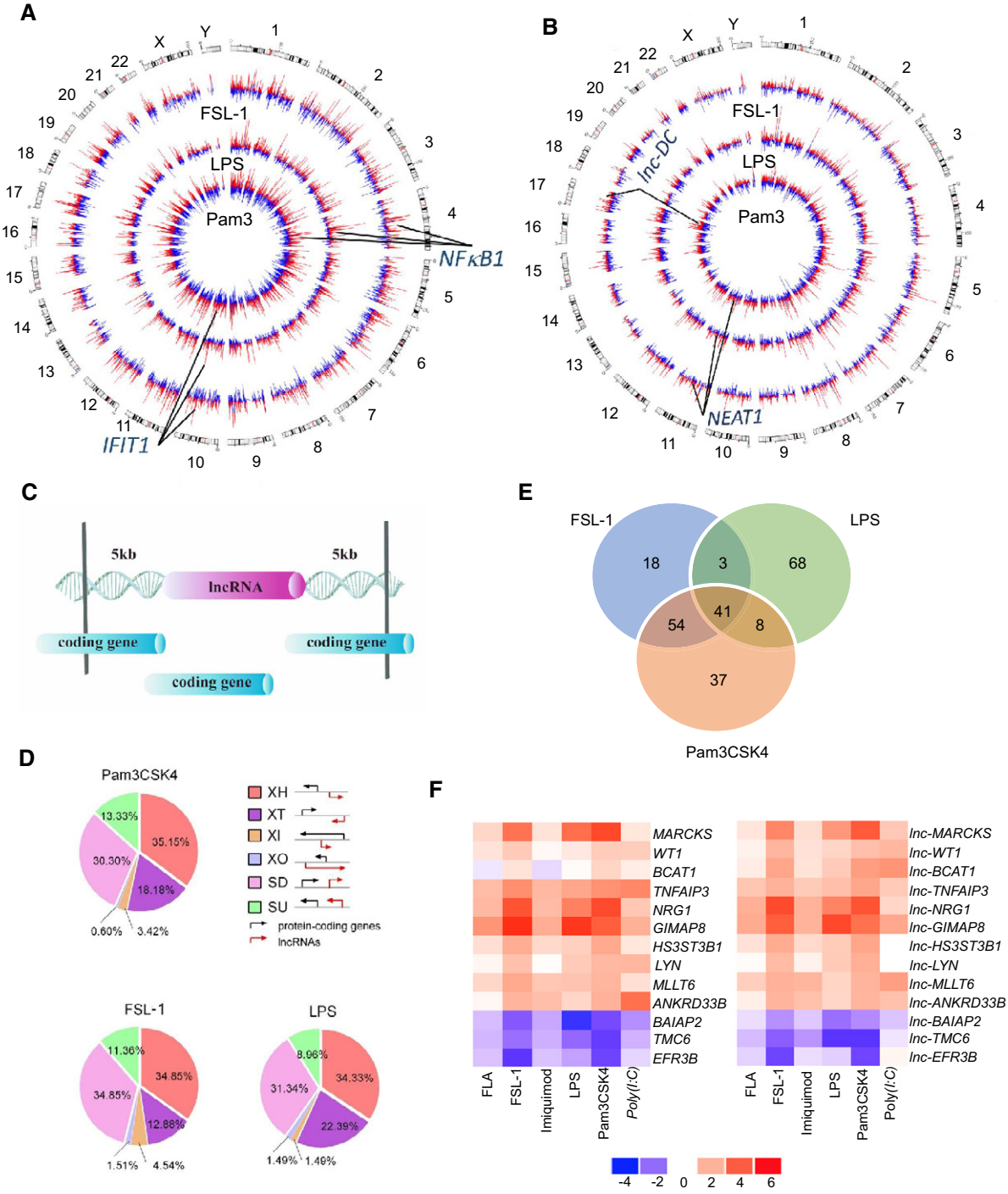

Figure 1. Identification of *cis*-acting LncRNAs associated with innate immunity.

A, B THP1-derived macrophages were treated with the TLR ligands Pam3, lipopolysaccharide (LPS), or FSL-1 and analyzed by RNA-seq 8 h later. Circos plots show genome-wide differential expression of protein-coding genes (A) and non-protein-coding genes (B) between untreated and treated macrophages. The outermost to innermost circles show downregulated (blue) or upregulated (red) genes in cells stimulated with FSL-1, LPS, and Pam3, respectively. Chromosomes are indicated by the numbers 1–22 and X and Y.

C Schematic showing *cis*-acting lncRNAs and protein-coding genes within 5 kb.

D Classification of lncRNA- and protein-coding gene pairs modulated by TLR ligands according to their biotypes. Pie charts show the proportion of each pair of genes classified as XH (antisense head-to-head), XT (antisense tail-to-tail), XI (antisense inside), XO (antisense outside), SD (sense downstream), and SU (sense upstream).

E LncRNA- and protein-coding gene pairs commonly upregulated or downregulated in THP-1-derived macrophages stimulated with FSL-1, LPS, or Pam3 for 8 h.

F RT–qPCR validation of differentially expressed lncRNAs and mRNAs in THP1-derived macrophages stimulated for 8 h with flagellin (FLA), FSL-1, imiquimod, LPS, Pam3, or poly(I:C). Heat map shows the fold change in expression of 13 mRNAs (left) and lncRNAs (right).

were found to be potential *cis*-regulators of 1, 2, and 3 protein-coding genes, respectively (Table EV1). We further classified these lncRNAs into six locus biotypes based on their orientation to the protein-coding gene (Fig 1D): XH, antisense head-to-head; XT, antisense tail-to-tail; XI, antisense inside; XO, antisense outside; SD, sense downstream; and SU, sense upstream, as described previously (Luo *et al*, 2016). The largest lncRNA biotype modulated by the TLRs was divergent XH, comprising 35.15, 34.85, and 34.33% of total lncRNAs differentially expressed in Pam3-, FSL-1-, and LPS-stimulated THP1-derived macrophages, respectively (Fig 1D). These results indicate that a large number of *cis*-acting lncRNA genes are non-randomly distributed in the genome and potentially play a role in regulating innate immune responses.

Cis-acting LncRNAs regulate expression of nearby protein-coding genes

To narrow down our functional analyses, we analyzed the 41 gene pairs commonly regulated by Pam3, LPS, and FSL-1 (Figs 1E and EV1D–F) and selected the 13 most differentially expressed pairs ($\log_2$-fold change in expression of > 2 or < -2), 10 of which were upregulated and 3 were downregulated. We then validated their differential expression by RT–qPCR of FSL-1, LPS- and Pam3-treated THP1-derived macrophages (Fig 1F). To determine whether these gene pairs were modulated by other TLRs, we also analyzed their expression in cells stimulated with *Salmonella Typhimurium* flagellin (FLA), poly(I:C), and imiquimod, which are TLR5, 3, and 7 ligands, respectively. Notably, the 13 gene pairs showed similar patterns of expression in response to all six TLR ligands (Fig 1F), supporting their potential importance in innate immunity.

Next, we examined the effects of the *cis*-acting regulatory lncRNAs on their cognate protein-coding genes. lncRNA expression was silenced in THP1-derived macrophages by infection with lentiviruses encoding control or targeted shRNAs for 4 days, and relative gene expression was analyzed by RT–qPCR. We used a pool of 2–5 shRNAs per lncRNA, each targeting different gene regions, to eliminate potential off-target effects and to enhance the knockdown (KD) efficiency. Of the 13 gene pairs examined, eight pairs were confirmed to have a *cis*-regulatory relationship (Fig 2A). Macrophages depleted of *lnc-MARCKS* and *lnc-BCAT1* showed significantly enhanced expression of the protein-coding genes *MARCKS*, and *BCAT1*, respectively, compared with control shRNA-expressing cells, which confirmed that these lncRNAs are negative regulators of the linked genes. *lnc-WT1* showed a moderate effect to negatively regulate *WT1* gene (Fig 2A). In contrast, KD of *lnc-ANKRD33B*, *lnc-BAIAP2*, *lnc-TNFAIP3*, *lnc-TMC6*, and *lnc-NRG1* significantly reduced expression of the cognate protein-coding genes, suggesting that these are positive *cis*-regulatory lncRNAs (Fig 2A). *lnc-BCAT1*, *lnc-WT1*, *lnc-BAIAP2*, and *lnc-TNFAIP3* were identified as XH lncRNAs (antisense head-to-head), *lnc-MARCKS* as an XT lncRNA (antisense tail-to-tail), and *lnc-TMC6*, *lnc-ANKRD33B*, and *lnc-NRG1* as SD lncRNAs (sense downstream) (Figs 1D and 2A).

Characterization of the *cis*-regulatory LncRNAs

Because most of the lncRNAs identified here were annotated based on bioinformatics predictions, we performed rapid amplification of cDNA ends (RACE) to confirm their location and to determine the 5′ and 3′ end sequences of the uncharacterized lncRNAs. From these experiments, we found that *lnc-ANKRD33B* and *lnc-NRG1*, which were predicted to be in the sense strand overlapping the corresponding protein-coding genes, were in fact isoforms of the protein-coding genes. *lnc-MARCKS*, *lnc-BCAT1*, *lnc-BAIAP2*, and *lnc-TNFAIP3* were confirmed to be *bona fide* transcripts, and the predicted sequences were authenticated (Fig EV2A). We identified two isoforms of *lnc-BAIAP2* and *lnc-TNFAIP3* and only one form of *lnc-MARCKS* and *lnc-BCAT1* (Fig EV2A). Thus, among the 13 gene pairs functionally tested here, 6 (46%) included *cis*-acting lncRNAs. This demonstrates the power of our prediction methods to identify *cis*-acting lncRNAs. Interestingly, five of the six lncRNAs were antisense to their protein-coding genes, strongly suggesting that divergent (XH and XT) biotypes are enriched among *cis*-acting lncRNAs.

Cis-acting LncRNAs regulate cytokine production in response to group B streptococcus (GBS) infection

To confirm the relevance of the identified gene pairs in the response to live bacterial infection, we used the Gram-positive pathogen GBS as a model system to activate TLR2 signaling (Lehnardt *et al*, 2006; Henneke *et al*, 2008). THP1-derived macrophages were infected with pooled lentiviruses encoding 2–5 shRNAs against *lnc-BAIAP2*, *lnc-MARCKS*, *lnc-WT1*, *lnc-BCAT1*, *lnc-TMC6*, or their corresponding protein-coding genes *BAIAP2*, *MARCKS*, *WT1*, *BCAT1*, or *TMC6*. All gene pairs were shown by RT–qPCR to be silenced with good efficiencies (Fig EV2B). Three days later, the cells were infected with GBS (multiplicity of infection = 10 bacteria/macrophage) for 1 h, after which gentamicin was added to kill extracellular bacteria, and the cells were collected for RT–qPCR analysis 10 h later. Expression of *IL-6* and *IL-1α*, two potent proinflammatory genes induced by GBS infection, was significantly enhanced by KD of *BAIAP2*, *lnc-BAIAP2*, *MARCKS*, WT1, and BCAT1 and significantly suppressed by KD of *lnc-MARCKS* and *lnc-BCAT1* (Fig 2B–D). Although KD of *lnc-WT* or *lnc-TMC6* also had modest effects on IL-6 expression, the differences were not statistically significant (Fig 2C). These results substantiate the predicted mode of action of *lnc-BAIAP2* as a positive *cis*-regulator and of *lnc-MARCKS* and *lnc-BCAT1* as negative *cis*-regulators of their corresponding protein-coding genes. The data also confirm the involvement of these three gene pairs in regulating proinflammatory cytokine expression during GBS infection.

The long noncoding RNA, *lnc-MARCKS*, is a positive regulator of inflammatory responses

We observed a global regulation of *lnc-MARCKS* on other cytokine and chemokine expressions, such as *CXCL1*, *IL-24*, and *CCL3* (Figs 1F and 2B–D, see below Fig 6), suggesting its role as a master regulator of innate immunity. Therefore, *lnc-MARCKS* was chosen for further investigation.

To determine the *lnc-MARCKS* function by an alternative approach, THP1 cells were transduced with CRISPR inhibitor system (CRISPRi) targeting *lnc-MARCKS* (Gilbert *et al*, 2013). Two sgRNAs were designed to target *lnc-MARCKS* (Fig 3A) and > 80% inhibition of *lnc-MARCKS* was achieved (Fig 3B). Consistent with the results of

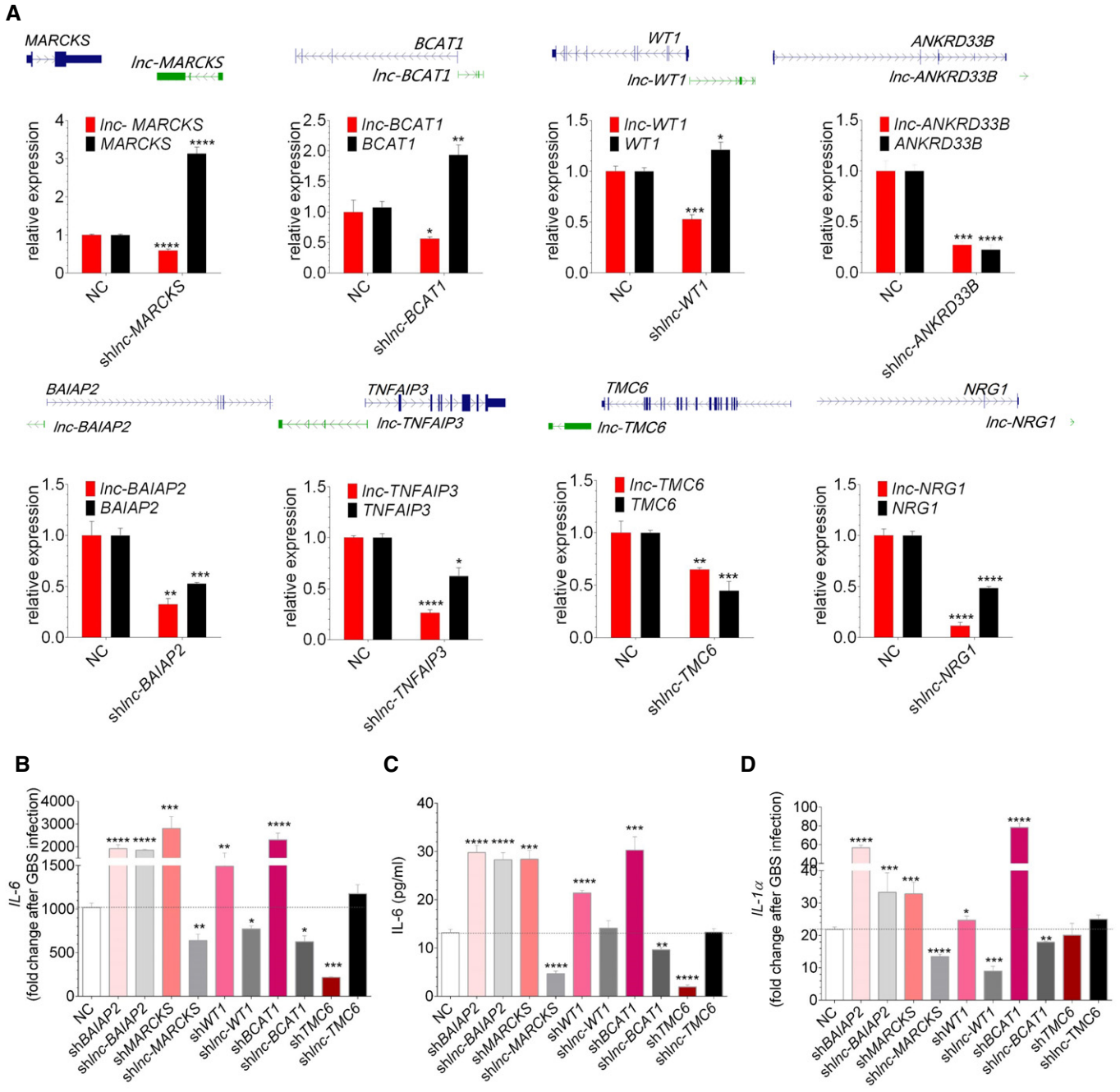

Figure 2. *Cis*-acting LncRNAs regulate nearby genes and cytokine production in response to group B *Streptococcus* (GBS) infection.

A Activation and suppression of nearby genes by eight *cis*-acting lncRNAs. RT–qPCR analysis of THP1-derived macrophages transduced with lentiviruses expressing non-targeting control (NC) shRNA or shRNAs targeted to the indicated lncRNAs and protein-coding genes. Mean ± SD of $n = 3$. *$P < 0.05$, **$P < 0.01$, ***$P < 0.005$, ****$P < 0.0001$ by Student's *t*-test.

B–D Silencing of *cis*-regulated gene pairs affects GBS-induced expression of IL-6 (B and C) and IL-1α (D). RT–qPCR analysis (B and D) or IL-6 ELISA quantification (C) of THP1-derived macrophages transduced with the indicated NC or targeting shRNAs for 72 h, infected with GBS for 1 h, and then treated with gentamicin for 30 min to terminate infection. RT–qPCR and ELISA were performed at 10 h post-infection. Mean ± SD of $n = 3$. *$P < 0.05$, **$P < 0.01$, ***$P < 0.005$, ****$P < 0.0001$ by Student's *t*-test.

our functional analysis by RNAi (Fig 2B–D), CRISPRi of *lnc-MARCKS* increased *MARCKS* expression (Fig 3C) and caused repression of *IL-6* induction in sgRNA-expressed cells (Fig 3D), indicating that *lnc-MARCKS* was a negative regulator of *MARCKS* and positive regulator of inflammation responses. Additionally, overexpression of an approximately 2.7-kb transcript of *lnc-MARCKS* (identified by RACE; Fig 3E) in THP1-derived macrophages significantly downregulated basal *MARCKS* mRNA (Fig 3F) levels and increased *IL-6*

mRNA levels upon Pam3 stimulation (Fig 3G). Further characterization showed that the *lnc-MARCKS* RNA was present in THP1 macrophages at ~6 copies per cell and mainly distributed in nucleus (Fig EV3A). A small proportion of lncRNAs undergo translation and could encode stable and functional peptides (Housman & Ulitsky, 2016; Hezroni *et al*, 2017). To determine whether *lnc-MARCKS* lacks protein-coding potential or not, we predicted the possible proteins in *lnc-MARCKS* using SnapGene software and found one ORF (93aa) near the 3′-end. However, the coding product cannot be aligned to any known proteins (Fig EV3B). These analyses suggested that *lnc-MARCKS* did not code for small peptides. In addition, ribosome footprinting data from GWIPS shows very weak ribosomal binding on *lnc-MARCKS*, which suggest that *lnc-MARCKS* is a noncoding RNA (Fig EV3C) (Ingolia *et al*, 2009). To further confirm the noncoding potential of *lnc-MARCKS*, we fused *lnc-MARCKS* sequences to the reading frame of a Flag tag and transfected the vectors into 293T cells. Notably, anti-Flag Western blot analysis failed to detect any protein expression from the constructs, confirming that *lnc-MARCKS* is a *bona fide* noncoding RNA (Fig EV3D).

To further strengthen the biological significance of *lnc-MARCKS*, we generated primary human macrophages and silenced *lncRNA-MARCKS* expression by using an antisense oligo targeting the RNA

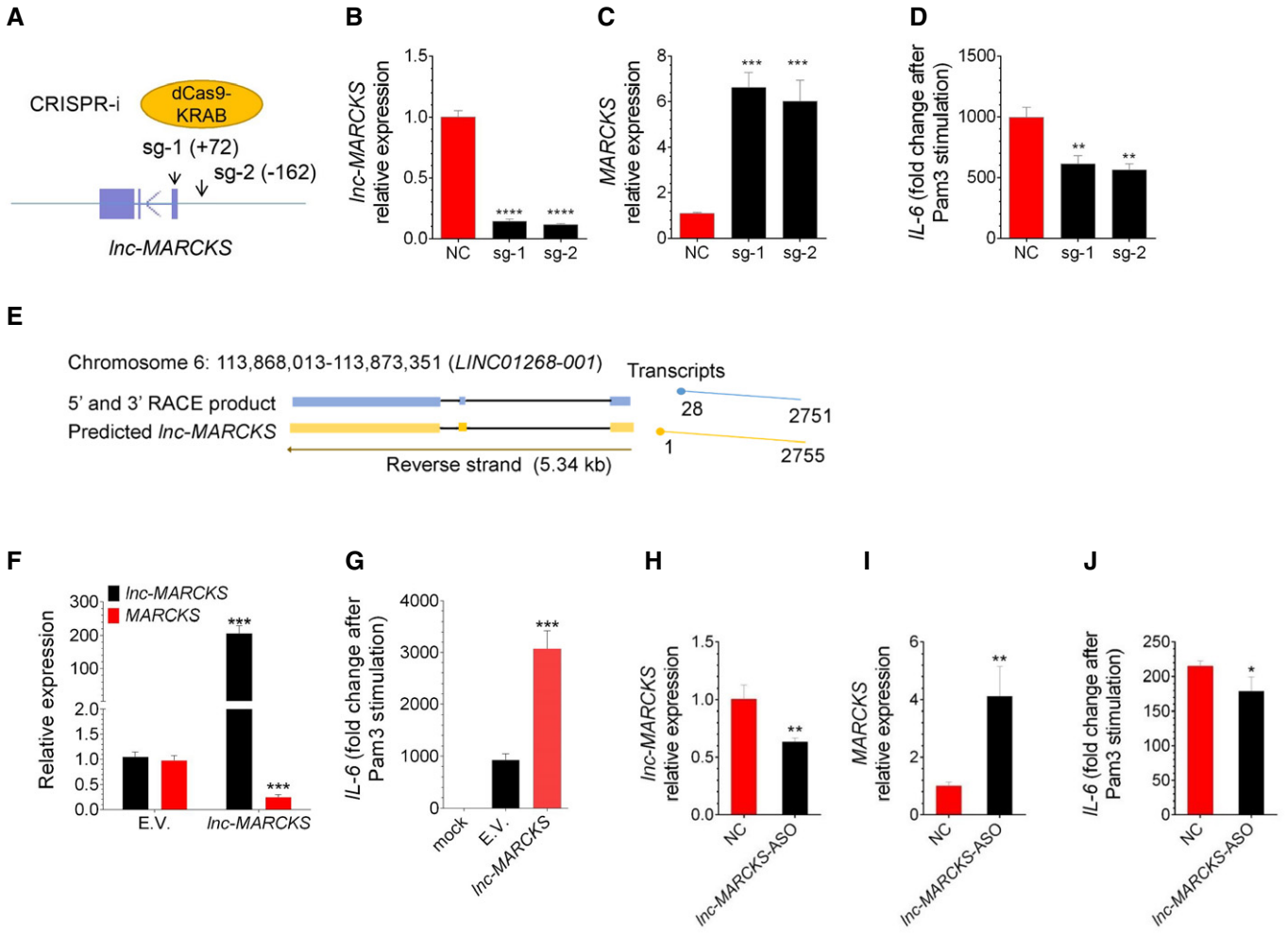

Figure 3. *lnc-MARCKS* negatively regulates *MARCKS* expression and promotes inflammatory responses.

A–D Repression of *lnc-MARCKS* using CRISPRi increased *MARCKS* expression and decreased *IL-6* induction. (A) Illustration of CRISPRi system and the relative locations of the two sgRNAs. (B-D) *lnc-MARCKS* (B), *MARCKS* (C), and *IL-6* (D) expressions were quantified in cells stably expressing dCas9/KRAB/BFP and the NC or sgRNAs. Mean ± SD of $n = 3$. $^{**}P < 0.01$, $^{***}P < 0.005$, $^{****}P < 0.0001$ by Student's *t*-test.

E The *lnc-MARCKS* gene locus. The full-length sequence of *lnc-MARCKS* was obtained by rapid amplification of cDNA ends (RACE). *lnc-MARCKS* is located on human chromosome 6 and encompasses 2 exons.

F, G Overexpression of *lnc-MARCKS* decreases *MARCKS* expression and enhances *IL-6* expression. RT–qPCR analysis of THP1 cells transduced with lentiviruses expressing empty vector (E.V.) or *lnc-MARCKS*, treated with PMA overnight, and left unstimulated or stimulated with Pam3 for 8 h. *lnc-MARCKS* and *MARCKS* expression (F), *IL-6* expression (G). Mean ± SD of $n = 3$. $^{***}P < 0.005$ by Student's *t*-test.

H–J *lnc-MARCKS* regulates *MARCKS* and *IL-6* in primary macrophages. Primary macrophages were transfected with NC or *lnc-MARCKS* antisense oligo to knock down *lnc-MARCKS* expression. 48 h later, cells were stimulated with Pam3 for 8 h and harvested to detect *lnc-MARCKS* (H), *MARCKS* (I), and *IL-6* expressions (J). Mean ± SD of $n = 3$. $^{*}P < 0.05$, $^{**}P < 0.01$ by Student's *t*-test.

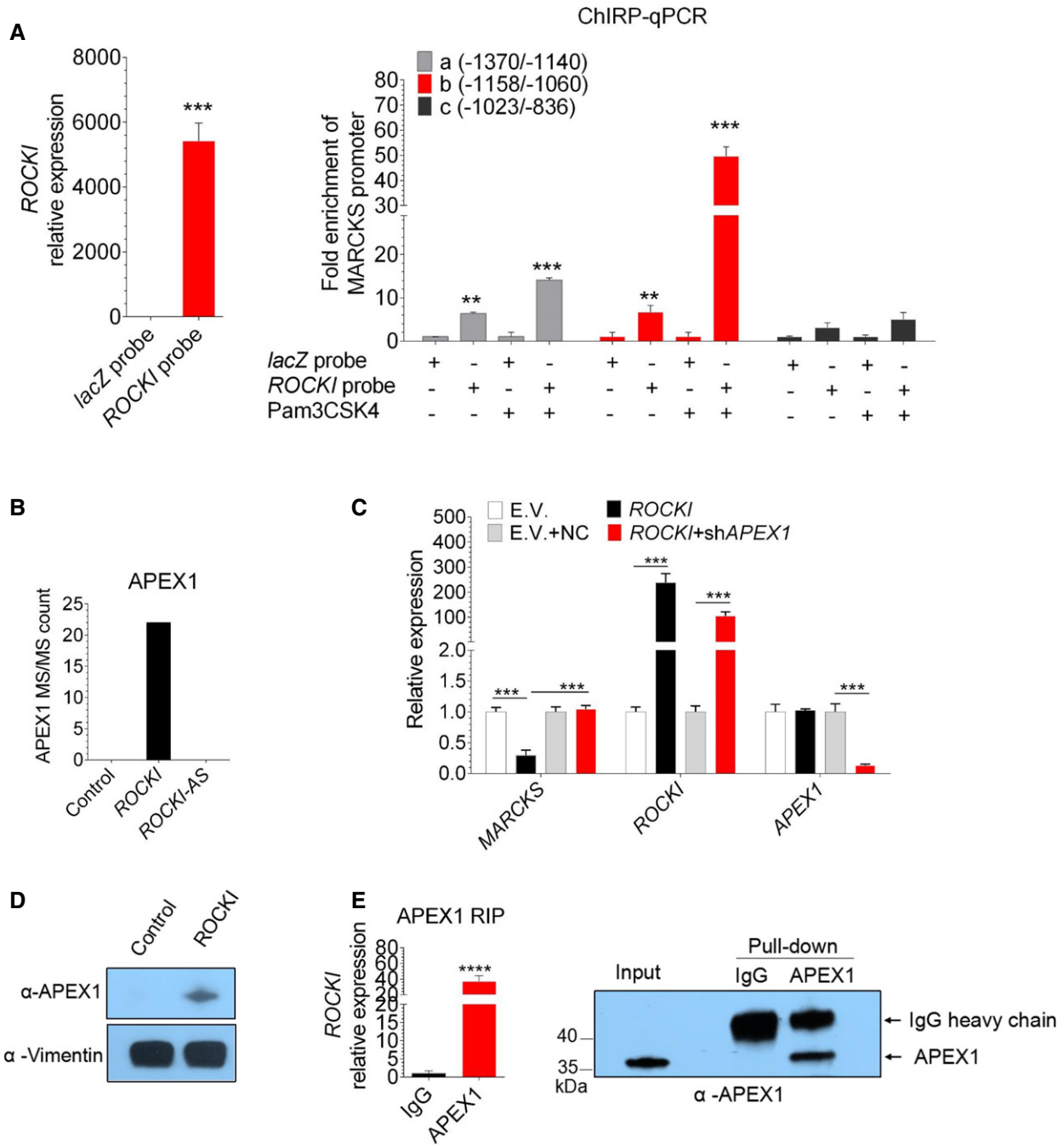

Figure 4. *ROCKI (lnc-MARCKS)* binds to the *MARCKS* Promoter and Interacts with APEX1.

A *ROCKI* is recruited to the *MARCKS* promoter in Pam3-stimulated THP1-derived macrophages. ChIRP analysis of THP1-derived macrophages treated with Pam3 for 8 h. ChIRP assays were performed using a non-specific *lacZ* probe or probes specific for *lnc-MARCKS*. Specificity of *ROCKI* probes (left), and enrichment at the *MARCKS* promoter (right). Probes are listed in Table EV2. Mean ± SD of $n = 3$. $^{**}P < 0.01$, $^{***}P < 0.005$ by Student's *t*-test.

B Mass spectrometry identifies APEX1 as a candidate *ROCKI*-binding protein in THP1-derived macrophages. APEX1 MS/MS count represents the ratio between the number of APEX1 peptides and all peptides detected. Mean of $n = 2$ samples. *ROCKI and ROCKI-AS* represent *ROCKI* and antisense strand of *ROCKI* transcripts, respectively.

C *ROCKI* inhibition of *MARCKS* expression is dependent on APEX1. RT–qPCR analysis of *MARCKS*, *ROCKI*, and *APEX1* expression in THP1-derived macrophages overexpressing *ROCKI* and/or depleted of *APEX1*. Mean ± SD of $n = 3$. $^{***}P < 0.001$ by Student's *t*-test.

D APEX1 specially binds to *ROCKI*. Western blot analysis of APEX1 in *lacZ*, or *ROCKI* pull-down fractions. Vimentin, which non-specifically binds to all RNA probes, is shown as a loading control.

E *ROCKI* associates with APEX1. Left: RT–qPCR analysis of *ROCKI* present in anti-APEX1 antibody or control IgG immunoprecipitates from nuclear lysates of Pam3-treated THP1-derived macrophages. Right: APEX1 Western blot of the same immunoprecipitates. Mean ± SD of $n = 4$. $^{****}P < 0.0001$ by Student's *t*-test.

Source data are available online for this figure.

region at 1,887–1,907 nucleotides. Consistent with the shRNA and CRISPRi results (Figs 2B–D and 3A–D), *lnc-MARCKS* silencing by ASO increased *MARCKS* expression and repressed *IL-6* induction as compared with cells transfected with a control ASO (Fig 3H–J). Taken together, these results identify *lnc-MARCKS* as a positive regulator of the inflammatory macrophage response. Therefore, we re-named this lncRNA *ROCKI* (Regulator of Cytokines and Inflammation).

ROCKI functions by binding to the *MARCKS* distal promoter where it interacts with APEX1

To investigate the mechanism by which *ROCKI cis*-regulates *MARCKS* expression, we first performed chromatin isolation by RNA purification (ChIRP) assays to assess *ROCKI* binding to the *MARCKS* promoter. For this, we used an antisense oligonucleotide tiling method that encompassed the entire *ROCKI* sequence (Li *et al*, 2014; Lin *et al*, 2014). Chromatin fractions from control or Pam3-treated THP1-derived macrophages were incubated with biotinylated *ROCKI* or control (*lacZ*) RNA probes and analyzed by RT–qPCR for the presence of *MARCKS* promoter regulatory sequences. We designed six PCR primers spanning from −1,370 to +87 relative to the +1 transcription start site. By analogy to the conserved murine *MARCKS* sequence, this region was expected to include a distal promoter and a core promoter (Harlan *et al*, 1991; Wang *et al*, 2002). We observed that biotinylated *ROCKI* was significantly enriched compared to the control probe (Fig 4A, left). Importantly, RT–qPCR analysis of the sequences pulled down with *ROCKI* showed specific enrichment of the −1,370/−1,140 and −1,158/−1,060 *MARCKS* promoter sequences, indicating that *ROCKI* bound to the distal, rather than the proximal, promoter (Fig 4A).

We next asked whether *ROCKI* acted alone at the *MARCKS* promoter or might functions as part of an RNP. To identify *ROCKI*-binding proteins, we *in vitro*-transcribed and biotinylated *ROCKI*, antisense *ROCKI,* or a partial *lacZ* mRNA sequence (without protein-coding capacity) and incubated them with nuclear proteins isolated from Pam3-treated THP1-derived macrophages. The associated proteins were then pulled down and analyzed by mass spectrometry. We identified the 10 most enriched *ROCKI*-binding proteins as APEX1 (apurinic/apyrimidinic endodeoxyribonuclease 1), NUDT21 (NUDIX Hydrolase 21), RCC2 (regulator of chromosome condensation 2), HMGB2 (high mobility group box 2), HMGB3 (high mobility group box 3), HSD17B4 (hydroxysteroid 17-beta dehydrogenase 4), KHSRP (KH-type splicing regulatory protein), NCL (neuronal ceroid lipofuscinoses), CIRBP (cold-Inducible RNA binding protein), and ELAVL1 (ELAV like RNA binding protein 1) based on the number of peptides specifically associated with *ROCKI* (Figs 4B and EV4A, Table EV3).

To determine whether these candidate *ROCKI*-binding proteins function in regulating *MARCKS* expression, we transfected THP1-derived macrophages with shRNAs against each gene and performed RT–qPCR analysis to confirm they were efficiently knocked down (Fig EV4C). Among the 10 genes examined, silencing of APEX1 alone significantly affected *MARCKS* expression, inducing ~2-fold increase in the level of *MARCKS* transcripts compared with the control shRNA-transfected cells (Fig EV4B). Notably, *ROCKI*-induced suppression of *MARCKS* inhibition was rescued by co-transfection of THP1-derived macrophages with shAPEX1, indicating that *ROCKI*-mediated inhibition of *MARCKS* expression was dependent on APEX1 (Fig 4C).

We also performed pull-down assays with *in vitro*-transcribed biotinylated *ROCKI* or *lacZ* RNA followed by Western blotting with anti-APEX1 antibody, which confirmed that APEX1 specifically interacts with *ROCKI* (Fig 4D). To further confirm the APEX1-RNA interactions by an alternative experiment, we performed immunoprecipitation of endogenous APEX1 from nuclear extracts of THP1-derived macrophages followed by RT–qPCR and the results revealed ~40-fold enrichment of *ROCKI* in the anti-APEX1 immunoprecipitates compared to the IgG control (Fig 4E). Taken together, these results demonstrate that *ROCKI* and APEX1 form an RNP complex that regulates *MARCKS* expression.

ROCKI–APEX1 ribonucleoprotein complex facilitates HDAC1-mediated remodeling of the *MARCKS* promoter

Next, we sought to understand how the *ROCKI*–APEX1 complex regulates *MARCKS* expression. We hypothesized that *ROCKI* may recruit APEX1 to the *MARCKS* promoter. To test this, we performed chromatin immunoprecipitation (ChIP) assays by immunoprecipitating endogenous APEX1 protein from nuclear lysates of THP1-derived macrophages, eluting the associated DNA, and performing RT–qPCR analysis to probe for the presence of *MARCKS* promoter sequences. Indeed, APEX1 immunoprecipitates contained higher levels of the two *MARCKS* promoter sequences tested compared with control IgG immunoprecipitates (Fig 5A). Since APEX1 enrichment was impaired in *ROCKI* KD cells (Fig 5B), these data support our hypothesis that *ROCKI* recruits APEX1 to form an RNP at the *MARCKS* promoter. Importantly, *ROCKI* KD had no significant effect on APEX1 binding to the β-actin promoter (*ACTB2*), highlighting the specific function of *ROCKI*–APEX1 in regulating *MARCKS* expression (Fig 5B).

APEX1 is known to repress expression of human parathyroid hormone and renin by binding to the negative regulatory calcium-response element in the promoters and recruiting HDAC1, which removes the activating chromatin mark H3K27ac3 and reduces gene transcription (Bhakat *et al*, 2003; Fuchs *et al*, 2003). To determine whether APEX1 might act similarly to suppress *MARCKS* transcription, we first performed Western blotting to probe for the presence of HDAC1 in anti-APEX1 immunoprecipitates from nuclear lysates of control or sh*ROCKI*-expressing THP1-derived macrophages. These results show that HDAC1 associates with APEX1 in the nucleus and this interaction was not dependent on *ROCKI* expression (Fig 5C, left). RT–qPCR was performed to show the successful pull down of *ROCKI* in APEX1 immunoprecipitates and successful silencing in *ROCKI*-knockdown cells (Fig 5C right). We next analyzed the level of HDAC1 and H3K27ac at the *MARCKS* promoter in these cells by performing ChIP assays with an anti-HDAC1 or anti-H3K27ac antibody (Fig 5D and E). As expected, HDAC1 and H3K27ac immunoprecipitates were enriched in the two *MARCKS* promoter sequences and the *ACTB2* sequence, but only *MARCKS* sequence enrichment was significantly decreased in HDAC1-CHIP (Fig 5D), while increased in H3K27ac-CHIP (Fig 5E) by *ROCKI* KD. Taken together, these results show that *ROCKI* interacts with APEX1 to recruit HDAC1 to the *MARCKS* promoter, leading to a reduction in H3K27ac and repression of *MARCKS* transcription.

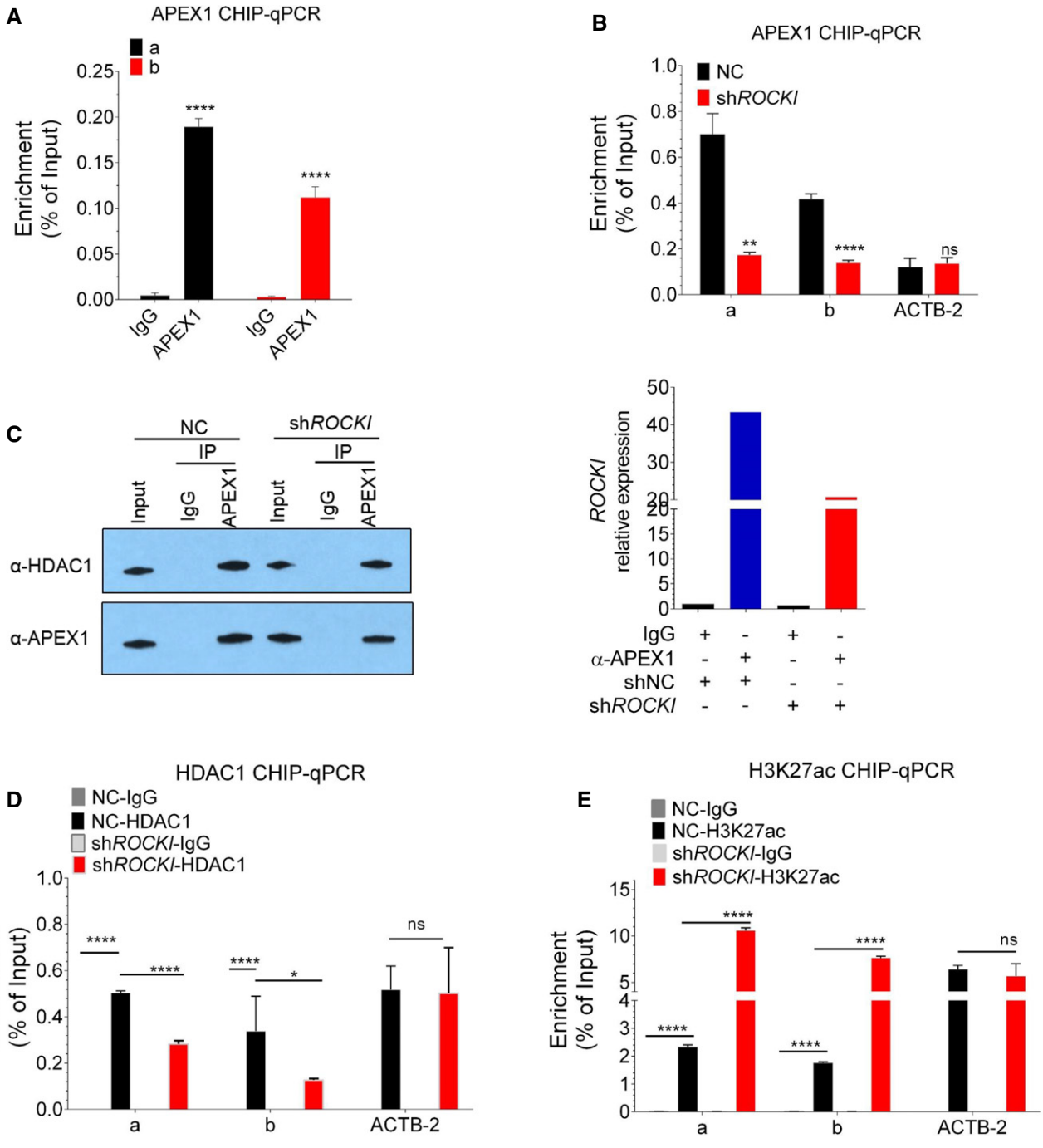

Figure 5. *ROCKI* reduces H3K27ac modification of the *MARCKS* promoter via APEX1 binding and recruitment of HDAC1.

A ChIP analysis of THP1-derived macrophages demonstrates APEX1 recruitment to the *MARCKS* promoter. RT–qPCR analysis of fragments of the *MARCKS* promoter region (a and b) or a non-specific region (nc) co-immunoprecipitated with anti-APEX1 antibody. Mean ± SD of $n = 4$. ****$P < 0.0001$ by Student's *t*-test.

B ChIP analysis of APEX1 recruitment to the *MARCKS* promoter was performed as described for (A) except the cells expressed non-targeting control (NC) or *ROCKI* shRNA and treated with Pam3 for 8 h. The *y*-axis shows the percentage of enrichment in normalized to input. An unrelated region of the *ACTB2* promoter was amplified as a control. Mean ± SD of $n = 4$. **$P < 0.01$. ****$P < 0.0001$, ns, non-significant by Student's *t*-test.

C Left: Western blot analysis of APEX1 and HDAC1 in control rabbit IgG or anti-APEX1 antibody immunoprecipitates from NC (control) or *ROCKI*-knockdown THP1-derived macrophages. Right: RT–qPCR analysis of *ROCKI* in the same immunoprecipitates.

D Knockdown of *ROCKI* decreased HDAC1 enrichment on the *MARCKS* promoter. ChIP-qPCR analysis of HDAC1 was performed as described for (A) using an anti-HDAC1 antibody. Mean ± SD of $n = 3$. *$P < 0.05$, ****$P < 0.0001$, ns, non-significant by Student's *t*-test.

E Knockdown of *ROCKI* enhances H3K27ac deposition on the *MARCKS* promoter. ChIP-qPCR analysis of H3K27ac was performed as described for (A) using an anti-H3K27ac antibody. Mean ± SD of $n = 3$. ****$P < 0.0001$, ns, non-significant by Student's *t*-test.

Source data are available online for this figure.

ROCKI regulates proinflammatory gene expression

To investigate how the *ROCKI–APEX1–HDAC1–MARCKS* axis regulates the innate inflammatory response in THP1-derived macrophages, we performed genome-wide RNA sequencing and analyzed differential gene expression changes in *MARCKS* KD- or *ROCKI*-overexpressing cells after stimulation with Pam3 for 8 h. Genes differentially regulated by both *ROCKI* overexpression (800 upregulated and 1,435 downregulated) and *MARCKS* KD (219 upregulated and 294 downregulated) were selected based on a significant ($P < 0.05$) $\log_2$-fold change of > 1 or < -0.5. We identified 128 genes that were considered to be commonly upregulated by both *ROCKI* and *MARCKS*, while 154 genes were identified to be commonly downregulated (Fig 6A and Table EV4). Notably, Gene Ontology analysis showed that the upregulated genes were significantly enriched in terms related to inflammatory responses (Fig EV5A). Among the most significantly upregulated genes were multiple cytokines, chemokines, and migration factors (Fig 6B); of these genes, we confirmed the lncRNA effects on 10 by RT–qPCR (Fig 6C).

In addition, we observed that these commonly regulated genes are highly overlapped with immune pathways, including the IL-17 signaling pathway, IL-1 signaling in melanoma, and histamine H1 receptor signaling in immune responses (Fig EV5C). In the histamine H1 receptor signaling, Ca^{2+} initiates the inflammation response by binding to PKCα (Fig EV5C). Since MARCKS protein is a well-characterized modulator of Ca^{2+} signaling (Hartwig *et al*, 1992; Gadi *et al*, 2011; Rodriguez Pena *et al*, 2013) and APEX1 can be acetylated by calcium activation to modulate its transcriptional

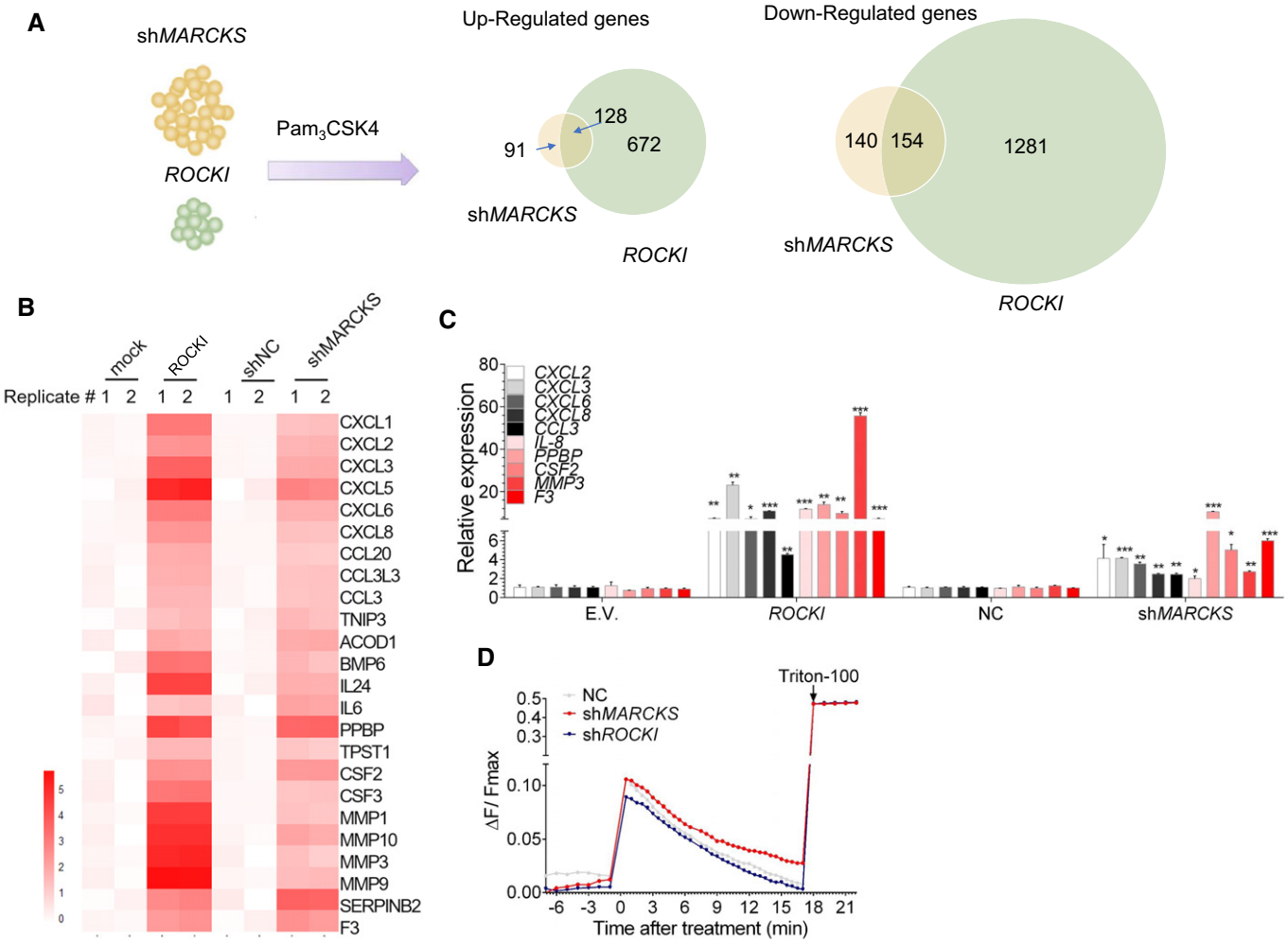

Figure 6. *ROCKI* and *MARCKS* are Ca^{2+} regulators in TLR1/2 signaling.

A Identification of genes regulated by both *ROCKI* and *MARCKS* by RNA-seq of *ROCKI*-overexpressing or *MARCKS*-knockdown THP1-derived macrophages stimulated with Pam3 for 8 h.

B Heatmap of representative genes commonly upregulated in *ROCKI*-overexpressing and *MARCKS*-knockdown THP1-derived macrophages.

C RT–qPCR validation of inflammatory gene expression in *ROCKI*-overexpressing and *MARCKS*-knockdown THP1-derived macrophages stimulated with Pam3 for 8 h. E.V., empty vector; NC, control shRNA. Mean ± SD of $n = 4$. *$P < 0.05$, **$P < 0.01$, ***$P < 0.001$ by Student's t-test.

D *MARCKS* is a negative regulator of Ca^{2+} signaling. Fluo-4 fluorescence of *MARCKS*, *ROCKI*, or NC (control) shRNA-expressing THP1-derived macrophages before and after treatment with PMA and Pam3. Triton X-100 was added to obtain the maximal $[Ca^{2+}]$ signal. Fluorescence levels are expressed as the change in signal normalized to the maximal fluorescence ($\Delta F/F_{max}$).

regulatory function (Bhakat *et al*, 2003, 2009), we asked whether it might play a similar role in Pam3-stimulated THP1-derived macrophages. To test this, we loaded cells expressing control, *MARCKS*, or *ROCKI* shRNA with the Ca^{2+}-sensitive fluorescent dye Fluo-4 and examined the change in fluorescence signal after Pam3 stimulation. As shown in Fig 6D, cytoplasmic Ca^{2+} levels were increased by *MARCKS* KD and decreased by *ROCKI* KD compared with control cells, suggesting that the *ROCKI–MARCKS* axis may regulate cytokine production in TLR-stimulated macrophages via Ca^{2+} signaling pathways.

Genetic links between *ROCKI* and inflammation- and infection-related phenotypes

Finally, we used genetic variation to explore whether *ROCKI* function is linked to human disease phenotypes. We first sought to

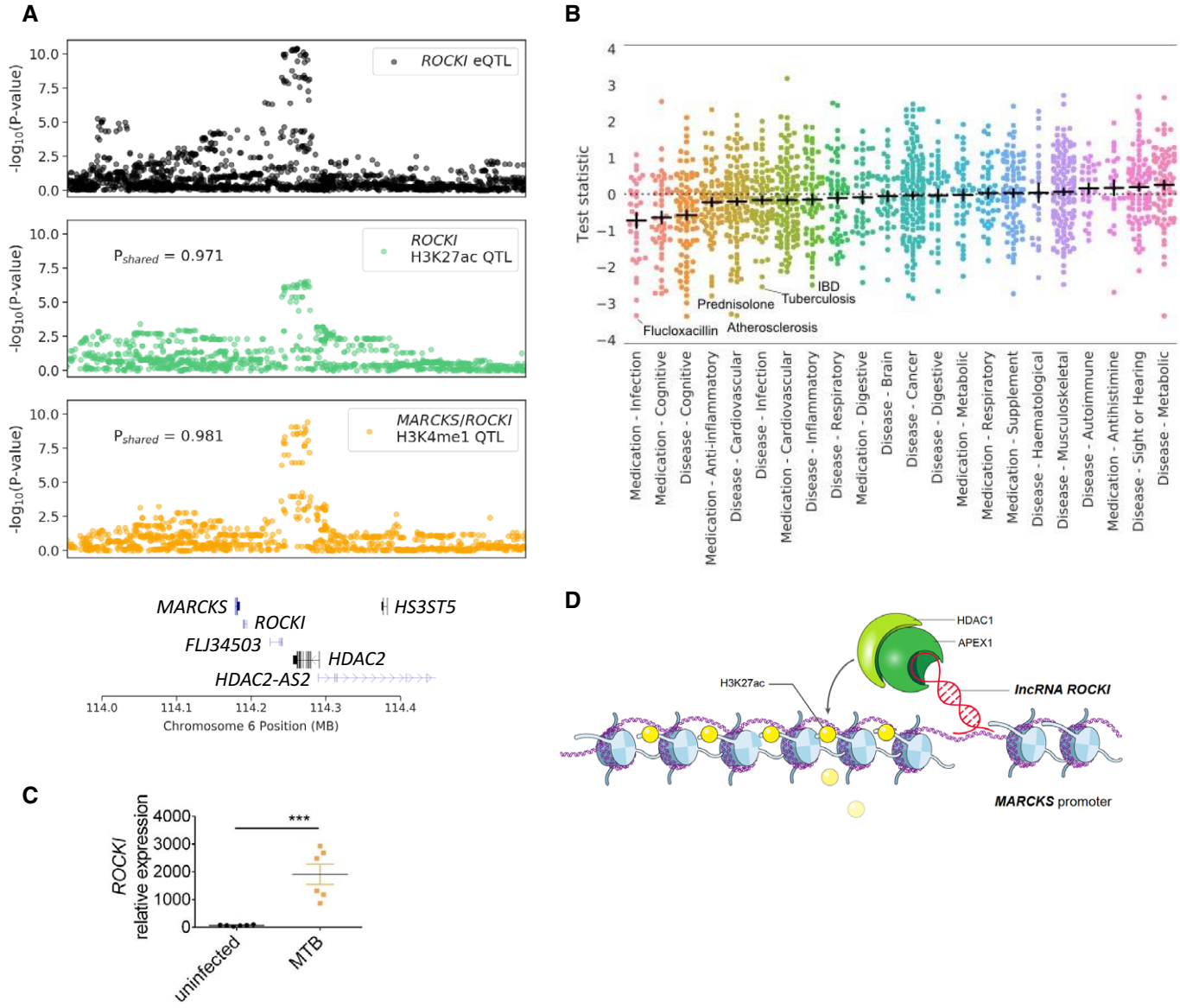

Figure 7. Genetic link between *ROCKI* and human disease and a model for *ROCKI* function.

A QTL signals for *ROCKI* (*LINC01268*) gene expression in whole blood (top, black), H3K27ac promoter signal in monocytes (middle, green), and H3K4me1 signal in monocytes (bottom, orange) in a 400-kb window around the *MARCKS*/*ROCKI* locus. The signals were strongly co-localized (P_{shared} = 0.97, P_{shared} = 0.98), suggesting they represent the same signal.

B Signed test statistics from UK Biobank association data for 1,463 disease- or medication-related traits for rs9387181. Black crosses denote the mean ± SEM for each group. Dotted horizontal line indicates the null.

C RT–qPCR analysis of *ROCKI* expression in dendritic cell samples from uninfected and *M. tuberculosis*-infected donors. Mean ± SD of n = 6. ***$P < 0.001$ by Student's t-test.

D A *cis*-regulatory model for *ROCKI* function in the negative regulation of *MARCKS* in innate immune cells. Upon TLR activation, *ROCKI* binds to the *MARCKS* promoter region and recruits APEX1, which facilitates HDAC1-mediated removal of the H3K27ac modification, thereby inhibiting *MARCKS* expression.

identify *cis* variants that affect *ROCKI* expression using quantitative trait loci (QTL) data. We obtained whole blood expression QTL (eQTL) data from the GTEx project v7 release (GTEx Consortium *et al*, 2017). There was a significant *ROCKI* eQTL for variants upstream of the promoter (Fig 7A). These variants did not show evidence for significant eQTL association with *MARCKS*, confirming a primary effect on *ROCKI* (Fig EV6A). To further determine the effects of these variants in monocytes, we analyzed $CD14^+$ monocyte QTL datasets for H3K4me1 and H3K27ac signal from the BLUEPRINT epigenome project (Chen *et al*, 2016). For the same *ROCKI* eQTL variants, there were also significant QTLs for H3K27ac signal directly at the *ROCKI* promoter and H3K4me1 signal in a broader 35-kb region spanning both *MARCKS* and *ROCKI* (Fig EV6). There was both strong co-localization and directional consistency in the *ROCKI* expression, H3K27ac, and H3K4me1 QTLs ($P_{shared} > .95$), suggesting they all represent the same association signal (Fig 7A). To determine the variant responsible for the *ROCKI* QTL, we performed genetic fine-mapping and calculated the posterior probability of association (PPA) that each variant was causal for the QTL signal (see Experimental Procedures). The most likely causal variant rs9387181 (PPA = 0.15) overlapped a regulatory region 6-kb upstream of *ROCKI* annotated with DNase I hypersensitivity sites for monocytes and ChIP-seq sites for immune transcription factors such as RELA and IRF4 (Fig EV6B). These data thus identify *cis*-regulatory variants that affect *ROCKI* activity in whole blood and monocytes.

We next determined the effects of the *ROCKI cis*-regulatory variants on human phenotypes. We obtained association data for 1464 disease-related phenotypes (UK Biobank) using the most probable *ROCKI* eQTL variant rs9387181 to represent the association signal. The *ROCKI*-reducing allele of rs9387181 was broadly correlated with reduced risk of inflammatory and infection-related, cardiovascular, and cognitive diseases and reduced use of the corresponding medications (Fig 7B). The most significant correlations for this variant within each group included reductions in flucloxacillin treatment ($t = -3.3$), prednisolone treatment ($t = -2.8$), atherosclerosis ($t = -2.99$), tuberculosis infection ($t = -2.5$), and inflammatory bowel disease ($t = -2.5$). These results thus provide genetic support for a link between *ROCKI* function in whole blood cells and isolated monocytes and the risk of inflammation- and infection-related disease phenotypes. To probe further, we analyzed data from a study of gene expression in human dendritic cells infected with *Mycobacterium tuberculosis* (Pacis *et al*, 2015). Intriguingly, *ROCKI* expression was significantly increased in the cells infected with *M. tuberculosis* (Fig 7C), confirming the predicted association.

Collectively, the data presented here demonstrate a role for the lncRNA *ROCKI* in innate immune function during human pathogen infection. Our data support a model in which *ROCKI cis*-regulates *MARCKS* expression via formation of an RNP with APEX1 at the *MARCKS* promoter, which facilitates HDAC1-mediated removal of H3K27ac, leading to reduced MARCKS expression and suppression of Ca^{2+} signaling and inflammatory cytokine production (Fig 7D).

Discussion

Activation of immune cells by pathogens leads to rapid and dynamic changes in gene expression aimed at combating the infection. Previous studies have demonstrated that the expression of hundreds of lncRNAs is altered by stimulation of innate and adaptive immune cells; however, their functions remain largely unknown (Carpenter *et al*, 2013; Rapicavoli *et al*, 2013; Li *et al*, 2014; Atianand *et al*, 2016; Wang *et al*, 2017). Here, we analyzed the expression of coding and noncoding genes in TLR-stimulated human macrophages to identify *cis*-regulatory lncRNAs and protein-coding genes. We identified 229 gene pairs with potential roles in immune regulation and selected 13 candidate pairs that were commonly regulated by six TLRs (TLR1/2, 2/6, 3, 4, 5, and 7) for functional validation. Eight lncRNAs were confirmed to *cis*-regulate their corresponding protein-coding genes. Of these, three (*ROCKI*, *lnc-BCAT1*, and *lnc-WT1*) were negative regulators and five (*lnc-ANKRD33B*, *lnc-NRG1*, *lnc-TMC6*, *lnc-BAIAP2*, and *lnc-TNFAIP3*) were positive regulators of their cognate genes. Further analysis showed that *lnc-ANKRD33B* and *lnc-NRG1* overlapped with and were assumed to be isoforms of their cognate coding genes. Interestingly, five of the remaining six lncRNAs had antisense biotypes (XH: *lnc-BCAT1*, *lnc-WT1*, *lnc-BAIAP2*, *lnc-TNFAIP3*, *and XT: ROCKI*). Antisense lncRNAs comprise over 90% of genic lncRNAs (lncRNA < 5 kb to a coding gene). Since > 60% of the 229 potential gene pairs identified here include antisense lncRNAs (Mancek-Keber *et al*, 2012; Lee *et al*, 2015), we expect that further mining of our data will reveal vital information about the landscape of functional lncRNAs in TLR signaling.

Activation of TLRs regulates immune responses through a highly controlled network of gene expression. Among the four functional lncRNA-gene pairs, *MARCKS*, *BCAT1*, and *WT1* were induced by TLR ligands, acts in a negative feedback manner to inhibit cytokine productions. These genes are "brakes" in controlling excessive immune response. In the meantime, *ROCKI*, *lnc-BCAT1*, and *lnc-WT1* were co-induced by stimuli, acting as a negative regulator of these brake genes to maintain the proper immune responses. *lnc-BAIAP2* positively regulated *BAIAP2* expression, and they were simultaneously decreased by TLR stimulus to promote immune response (Fig 2A–D). All these results confirmed that TLR pathways induce or suppress the expression of lncRNAs to turn on a lncRNA-directed regulatory circuit, contributing to stricter and tighter regulation of TLR network. The most abundant and promising antisense lncRNAs belong to XH group and their average distance between the nascent transcription start sites is ~800 bp, a distance that can be easily co-regulated on the genome. Local regulation of gene expression by *cis*-lncRNAs may involve regulatory components in gene promoters, the process of transcription or splicing, or the sequence/structure of the RNAs. Although *cis*-regulation by lncRNAs can be independent of the lncRNA transcripts themselves and could involve the RNA transcription and splicing mechanisms (Engreitz *et al*, 2016; Joung *et al*, 2017), but a number of studies showed that *cis*-regulatory functions of lncRNAs were dependent on the sequence/structure of the RNAs (reviewed in Guil & Esteller, 2012 and Kopp & Mendell, 2018). For example, a divergent lncRNA *Evx1 cis*-regulates adjacent coding genes based on its sequence during lineage differentiation in pluripotent cells (Luo *et al*, 2016). In our studies, *ROCKI* function was dependent upon the lncRNA sequence and ectopic expression enhanced inflammatory responses (Fig 3), representing an example of positive regulatory mechanism by lncRNA that is not a result of mere proximity of transcription.

We identified APEX1 as a *ROCKI*-binding protein; interestingly, this protein has previously been reported to regulate TLR2-dependent inflammatory responses in human keratinocytes (Lee *et al*, 2009). APEX1 can be acetylated by calcium activation to modulate its transcriptional regulatory function (Bhakat *et al*, 2003, 2009). Acetylated APEX1 binds more potently than the unacetylated protein to the parathyroid hormone promoter to repress its transcription (Bhakat *et al*, 2003). We observed a significant increase in *ROCKI* binding to the *MARCKS* promoter in Pam3-stimulated THP1-derived macrophages (Fig 4A). Further, APEX1 binding to *MARCKS* promoter was increased in Pam3-stimulated THP1-derived macrophages (Fig 5A and B) because Pam3 activates calcium, which leads to APEX1 acetylation and contributes to APEX1-*ROCKI* binding to the promoter. APEX1 was confirmed to recruit HDAC1 to modify histone acylation. We did not observe an enrichment of HDAC1 in our *in vitro* pull-down assay. There are two plausible explanations for this result: (i) This interaction is indirect binding, which is dependent on bridging of APEX1 as we proposed in our model Fig 7. (ii) This binding is temporal, thus hard to detect in the *in vitro* binding assay.

Several studies have identified a role for MARCKS in the regulation of inflammatory cytokine expression in myeloid cells. Treatment of neutrophils with LPS induces *MARCKS* expression and leads to its phosphorylation by protein kinase C (Aderem *et al*, 1988; Thelen *et al*, 1990; Seykora *et al*, 1991). Moreover, incubation of macrophages with peptides derived from the MARCKS effector domain not only blocked MARCKS phosphorylation and its disassociation from the membrane but also suppressed LPS-induced activation of p38, JNK, and NF-κB, thereby inhibiting inflammatory cytokine production (Lee *et al*, 2015). Another study proposed that MARCKS sequesters LPS to negatively regulate TLR4 signaling (Mancek-Keber *et al*, 2012). Here, we found that MARCKS expression was regulated not only by TLR4 but also by TLRs 1/2, 2/6, 2, 5, and 7, suggesting that it may be a master modulator of innate immune responses. Consistent with this, *MARCKS* KD and *ROCKI* overexpression increased the expression of dozens of inflammatory factors, including chemokines and cytokines (Figs 2 and 6). Interestingly, *ROCKI* overexpression regulated more genes involved in cytokine and inflammation than *MARCKS* KD, for example, *ILR2*, *IL1R1*, *CXCL16*, *CXCL12*, and *IL18BP* (Fig 6). A number of genes in MAPK pathway were also induced by *ROCKI* overexpression, such as *MAPKAPK2*, *MAPK10*, and *MAPKAPK3* (Table EV4). It remains to be determined whether *ROCKI* overexpression directly or indirectly affected genes which were not altered by *MARCKS* KD.

In addition, we observed that these commonly regulated genes highly overlapped with histamine H1 receptor signaling in immune responses (Fig EV5C). In the histamine H1 receptor signaling, Ca^{2+} initiates the inflammation response by binding to PKCα (Fig EV5C). Since MARCKS protein is a well-characterized modulator of Ca^{2+} signaling (Hartwig *et al*, 1992; Gadi *et al*, 2011; Rodriguez Pena *et al*, 2013), we propose that MARCKS regulates inflammation by controlling calcium release. As shown in Fig 6D, cytoplasmic Ca^{2+} levels were increased by *MARCKS* KD and decreased by *ROCKI* KD compared with control cells. Thus, modulating Ca^{2+} signaling pathways could be a new mechanism for MARCKS to regulate inflammation responses.

Taken together, our study developed a new strategy to illustrate lncRNAs with unknown function in TLR signaling. Importantly, we observed a genetic link between *ROCKI* activity in blood and monocytes and the risk of inflammation and infection-related disease phenotypes. We believe that our findings will help us understand the intact regulatory network of TLR signaling and also generate better experimental designs when investigating lncRNA transcripts in TLR signaling.

Materials and Methods

Cell culture

THP1 cells were cultured as described previously (Li *et al*, 2014). In brief, THP1 cells were cultured in RPMI 1640 medium supplemented with 10% fetal bovine serum (FBS) and 50 μM β-mercaptoethanol (Sigma). Cells were treated with 5 ng/ml phorbol-12-myristate-13-acetate (PMA) overnight to induce differentiation into macrophages, and the medium was replaced with PMA-free medium the following day. 293FT cells were cultured in DMEM supplemented with 10% FBS. Primary macrophages were generated by stimulating peripheral blood mononuclear cell (PBMC) with M-CSF (10 ng/ml, R&D) for 7 days in RPMI 1640 medium supplemented with 10% fetal bovine serum and 50 μM β-mercaptoethanol.

Bacterial culture

GBS (serotype IA strain A909) was cultured overnight at 37°C without shaking in Todd-Hewitt broth supplemented with 0.5% yeast extract. Bacteria were grown to logarithmic phase (OD = 0.4 or ~10 colony-forming units per ml), the centrifuged, washed, and resuspended in DMEM, and serially diluted to the desired concentration. For experiments, THP1-derived macrophages were inoculated with GBS at a multiplicity of infection of 10 bacteria per cell.

TLR ligand treatment

Human TLR agonists were purchased from Invivogen (# tlrl-kit1hw). Aliquots of 1×10^6 THP1-derived macrophages were seeded in 6-well plates and incubated with Pam3 (100 ng/ml), LPS (100 ng/ml), FSL-1 (100 ng/ml), flagellin (100 ng/ml), or imiquimod (5 μg/ml). For poly(I:C) stimulation, cells were transfected with 100 ng/ml poly(I:C) using Lipofectamine 3000 (Invitrogen) for 8 h. Cells were then washed with PBS and further processed as required for each experiment.

Interleukin-6 (IL-6) ELISA

In Fig 2C, the human Interleukin-6 ELISA kit (R&D, DY20605) was used for the quantitative determination of IL-6 expression in the supernatant of THP1 cells stimulated by GBS for 10 h. ELISA was performed following the protocol.

Library preparation and RNA-Seq

Approximately 0.5 μg total RNA per sample was depleted of ribosomal RNA using a RiboMinus kit (Life Technologies) and then processed using NEBNext Ultra RNA Library Prep Kit for Illumina

(New England BioLabs) with 15 cycles of PCR, according to the manufacturer's recommendations. The final libraries were size-selected on 2% agarose gels to obtain products between 280 and 380 bases in length. The libraries were loaded onto an Illumina HiSeq2000 for single-end 100 base-pair reads with 7 base index reads.

Lentiviral-mediated gene knockdown and *ROCKI* overexpression

shRNAs against protein-coding genes were purchased from the Functional Genomics Center (sequences listed in Table EV2). shRNAs against lncRNAs were designed using the open-access tool from the Broad Institute. Probes containing sense and antisense strands of shRNAs were annealed and cloned into pLKO.1 lentivirus vector (Addgene) following the manufacturer's instructions. *ROCKI* was cloned into a pFLAG-CMV plasmid for *ROCKI* overexpression experiments. Primer sequences for cloning shRNAs and *ROCKI* are listed in Table EV2. Lentiviruses were produced in 293FT cells using the protocol described previously (Khalil *et al*, 2009; Li *et al*, 2014). Briefly, aliquots of 1×10^6 cells/well were seeded into 6-well plates 1 day before transfection. The next day, lentiviral and packaging vectors (System Biosciences) were transfected into 293FT cells using Lipofectamine 2000 (Invitrogen) and virus-containing supernatants were collected 2 days after transfection. THP1 cells in 12-well plates (4×10^5/well) were transduced using 500 µl viral supernatant in the presence of 4 µg/ml polybrene, and 20 ng/ml PMA was added to induce differentiation. The transduction efficiency was enhanced by centrifuging the cell/virus mixture at 750 *g* for 45 min.

Primary macrophages transfection with antisense oligo (ASO)

PBMCs were seeded at 5 M/ml into 12-well plate. After 30 min, the suspending lymphocytes were removed and the remaining monocytes were changed to the M-CSF (10 ng/ml) containing medium. Media were changed every 2 days, and monocytes were differentiated into macrophages for 7 days. Next, transfection of 100 nM non-targeting ASO (CGACTATACGCGCAATATGG) or *ROCKI* ASO (TATATTTCAACCAGGAGGCAC) was performed using RNAiMAX (Thermo Fisher Scientific) for 48 h. After stimulation with Pam3 for additional 8 h, cells were harvested in TRIzol for detection of *ROCKI*, *MARCKS*, and *IL-6* expressions.

Repression of *ROCKI* expression using CRISPR inhibitor (CRISPRi)

For CRISPRi repression of *ROCKI*, we used the system that was previously established by Gilbert (Gilbert *et al*, 2013) with the following modifications. Briefly, polyclonal THP1 cells expressing dCas9/KRAB/BFP fusion proteins were generated by lentivirus transduction. Cells with higher BFP expression were sorted out. Two sgRNA oligos targeting ROCKI were designed and inserted into sgRNA expressing vector (lentiGuide-puro, Addgene 52963). Next, the vectors were packed into lentivirus and delivered into the sorted THP1- dCas9/KRAB/BFP cells. After 7 days of puromycin selection, cells were seeded and differentiated into macrophages, and stimulated with Pam3 for 8 h. The expressions of *ROCKI*, *MARCKS*, and *IL-6* were then determined using RT–PCR. sgRNA primers are listed in Table EV2.

RNA extraction and RT–qPCR

RNA was extracted from THP1 cells using TRIzol reagent (Invitrogen) according to the manufacturer's protocol. RNA was treated with DNase I (Ambion) to remove contaminating DNA, and samples of ~1 µg of RNA were reverse transcribed using Superscript III or VILO Mastermix (Invitrogen). qPCR was performed using SYBR Green mix or SsoAdvanced SYBR Green mix (Bio-Rad). The fold change in gene expression was calculated by the ΔΔCt method using glyceraldehyde 3-phosphate dehydrogenase (*GAPDH*) as an internal control. The primers used for qPCR are listed in Table EV2.

Rapid amplification of cDNA ends (RACE)

Total RNA was isolated from LPS-treated THP1 cells and processed with a Ribo-Zero-rRNA Removal kit to deplete ribosomal RNA (Epicentre). RACE was performed using a SMARTer RACE kit (Clontech) according to the user manual. Briefly, ~100 ng of purified poly(A) RNA was used for each RT reaction to produce lncRNA cDNA (20 µl), and nested PCRs were performed to amplify the lncRNA cDNA ends. Primer sequences for nested PCR reactions are listed in Table EV2. RACE PCR products were cloned using Zero Blunt TOPO cloning kit (Thermo Fisher Scientific) and then sequenced.

Chromatin isolation by RNA purification (ChIRP)

ROCKI binding to the MARCKS promoter was detected by ChIRP performed using 30 probes specific for *ROCKI*. The probes were designed using the online probe designer version 4.2 from LGC Biosearch Technologies. Masking level was set at 2, and the minimum spacing length was set at 60 nucleotides. Oligonucleotides were biotinylated at the 3′ end. THP1 cells were incubated in medium containing 20 ng/ml PMA for 18 h and then treated with or without 100 ng/ml Pam3 for 8 h. Cells were trypsinized, washed in medium, and then washed twice with PBS. Cells were fixed in 1% glutaraldehyde in PBS at room temperature for 10 min and then quenched with 1/10th volume of 1.25 M glycine for 5 min. Fixed cells were harvested by centrifuging at 2000 RCF for 5 min and washed twice with PBS. The cells were then lysed in lysis buffer (5 mM PIPES pH 8.0, 85 mM KCl, 0.5% NP-40), Dounce-homogenized 10 times on ice, and incubated for 10 min. Cell lysates were centrifuged at 2,500 *g* for 5 min at 4°C and the nuclear pellets were collected and sonicated (15 cycles, 30 s on, 30 s off). Isolated chromatin was analyzed for enrichment of *ROCKI* at the *MARCKS* promoter by ChIRP using the method described by Chu *et al* (2012). RT–qPCR primers are listed in Table EV2.

In vitro transcription and *ROCKI* RNA–protein pull-down assay

ROCKI, antisense of *ROCKI*, or *lacZ* control was cloned into pBluescript KSII downstream of the T7 promoter separately (primers listed in Table EV2). The vectors were linearized by KpnI digestion, and 1 µg of linear *lacZ*vectors was transcribed and biotinylated *in vitro* using a kit (Epicentre), according to the manufacturer's instructions. Biotinylated *RNAs* were purified, refolded, and incubated with nuclear lysates from THP1-derived macrophages using the method described previously (Li *et al*, 2014). Briefly, 2 µg of

diluted RNA (200 ng/μl) was incubated at 60°C for 10 min and slowly cooled to 4°C. Nuclear lysates were prepared from 2×10^8 PMA-differentiated THP1-derived macrophages treated with 100 ng/ml Pam3 for 8 h. Protein concentrations were measured by the DC assay (Bio-Rad) according to the manufacturer's instructions. For the pull-down incubations, nuclear lysates (1 mg of protein) were precleared with streptavidin beads (Invitrogen) and then incubated with 2 μg of biotinylated RNA and 40 μl of streptavidin beads for 2 h at 4°C. The beads were collected and washed three times with buffer C. RNA-associated proteins were eluted and analyzed by mass spectrometry (Sanford Burnham Prebys Medical Discovery Institute Core) or by Western blotting, as described below.

Reverse pull-down assays

To confirm that APEX1 binds to *ROCKI*, nuclear lysates (1 mg protein per sample) from 1×10^8 THP1-derived macrophages treated with Pam3 for 8 h were precleared with protein G beads (NEB) for 2 h at 4°C and then incubated with control rabbit IgG or anti-APEX1 antibody (4 μg per sample, Novus, NB100-101) overnight at 4°C. Protein G beads pre-blocked with bovine serum albumin were added to the samples for 2 h at 4°C, collected by centrifugation, washed three times with buffer C, and resuspended in 1 ml buffer C. RNA was extracted from 900 μl of each sample using TRIzol and treated with Turbo DNase to remove contaminating DNA. *ROCKI* levels were analyzed by RT–qPCR. The remaining 100 μl of each sample was collected, boiled for 5 min, and subjected to Western blot analysis to detect RNA-associated APEX1.

Chromatin immunoprecipitation (ChIP)

ChIP was performed using the method described by Deliard *et al* (2013) with minor modifications. Briefly, 2×10^7 THP1 macrophages were cross-linked with 1% formaldehyde for 10 min at room temperature and incubated with glycine for 5 min. Cells were collected by centrifugation, washed twice with PBS, lysed in lysis buffer, Dounce-homogenized 10 times on ice, and incubated for 10 min. The lysates were centrifuged at 4,000 rpm for 5 min at 4°C, and the nuclear pellets were resuspended in SDS lysis buffer and sonicated for 15 cycles (30 s on, 30 s off). DNA concentrations were quantified, and 10 μg of chromatin DNA was used for each ChIP reaction. ChIP assays were performed with 4 μg of antibody and 40 μl of protein G magnetic beads. The samples were incubated overnight at 4°C, washed, and eluted. Bead-bound DNA was reverse cross-linked and purified. RT–qPCR analysis was performed to detect the presence of two *MARCKS* promoter region sequences or an *ACTB2* sequence. *ACTB2* primers were purchased from Active Motif (71005). The antibodies used in these experiments include α-HDAC1 antibody (Abcam, ab7028), α-APEX1 (Novus, NB100-116), and α-H3K27ac (Abcam, ab4726).

Co-immunoprecipitation assay

To determine whether APEX1 and HDAC1 interact, APEX1 was immunoprecipitated as described for the reverse RNA pull-down assay. The beads were resuspended in 1 ml buffer C, and 900 μl was subjected to Western blot analysis of HDAC1 protein in the immunoprecipitates. The remaining 100 μl of sample was collected for RT–qPCR analysis of *ROCKI*.

Western blotting

Protein lysates were separated on 4–20% SDS/PAGE gels and transferred to PVDF membranes. Western blotting was performed using Fast Western Blot kits (Thermo Scientific Pierce) with the following antibodies: mouse anti-FLAG M2 antibody (Sigma, F1804), rabbit anti-glyceraldehyde 3-phosphate dehydrogenase (GAPDH; Cell Signaling Technology, 2118), rabbit anti-APEX1 (NOVUS, NB100-101), mouse anti-HDAC1 (NOVUS, NB100-56340SS), rabbit anti-H3K27ac (Cell Signaling Technology, 9733S), and mouse anti-vimentin (Abcam, ab8978).

Calcium flux assay

To detect changes in intracellular Ca^{2+} concentration in THP1-derived macrophages, 4×10^5 cells expressing control, *MARCKS*, or *ROCKI* shRNA were preincubated with the Ca^{2+} indicator Fluo-4 (Thermo Fisher, F14201) at 6 μM for 30 min, washed with Hanks' Balanced Salt Solution, and aliquoted into a 96-well plate at 4×10^4/well. Fluorescence signals were detected before and every 30 s after stimulation with PMA (50 ng/ml) and Pam3 (500 ng/ml). The maximal [Ca^{2+}] response was determined by adding 0.1% Triton X-100 to the cells at the end of the detection period. The change in fluorescence was normalized to the maximal fluorescence signal and is expressed as $\Delta F/F_{max}$.

MARCKS and *ROCKI* QTL analysis

Publicly available whole blood eQTL summary statistics were downloaded from the Genotype-Tissue Expression (Consortium *et al*, 2017) project v7 release (Consortium *et al*, 2017). We extracted all variants that were tested for association with *ROCKI* and *MARCKS* expression for further analysis. We also downloaded $CD14^+$ monocyte QTL summary statistic datasets for gene expression, H3K4me1, and H3K27ac from the BLUEPRINT epigenome project (Chen *et al*, 2016). The monocyte eQTL dataset could not be used in these analyses because it used an earlier release (GENCODE v15) for transcript annotation and *ROCKI* was not among the genes tested in this study. We extracted QTLs for H3K27ac and H3K4me1 signal in a genomic region around *MARCKS* and *ROCKI*.

For each dataset, we calculated Bayes factors for each variant in a 1 MB window around the signal following the approach of Wakefield (Wakefield, 2009). We then used a Bayesian co-localization method to determine whether the whole blood eQTL association for *ROCKI* and monocyte H3K27ac QTL association upstream of the *ROCKI* promoter and eQTL association for *MARCKS* showed evidence of a shared causal variant (Giambartolomei *et al*, 2014). We considered signals with a shared probability (P_{shared}) > 0.9.

We then performed fine-mapping to determine the causal variant for the shared signal using *ROCKI* eQTL and H3K27ac QTL data. For each variant in a 1 MB window around the signal and in common to both datasets, we multiplied Bayes factors for each signal and calculated a posterior probability of association (PPA) for each variant as the Bayes factor divided by the sum of Bayes

factors across all variants. We then intersected candidate casual variants with DNase I hypersensitivity sites (DHS) and transcription factor ChIP-seq sites from the ENCODE project (Maurano *et al*, 2012).

UK Biobank GWAS data analysis for phenotypic associations

Publicly available UK Biobank GWAS summary statistics for 2,419 phenotypes were downloaded (https://sites.google.com/broadinstitute.org/ukbbgwasresults). Phenotypes that did not appear to be related to diseases or disease treatments were removed, and we then extracted summary statistics for the most significantly associated *ROCKI* eQTL variant (rs9387181). For each phenotype, we aligned summary results to the *ROCKI*-reducing allele of rs9387181. We then categorized 1,464 disease- and medication-related phenotypes into 22 groups, removing phenotypes that did not fit in a clear group. We then plotted the signed test statistic of phenotypes within each group, and the average signed test statistic within each group.

Statistical analysis

Differences between groups were analyzed using Student's *t*-test (paired, two-sided). Data are presented as the mean ± standard deviation (SD). $N = 3$. Differences were considered statistically significant when $P < 0.05$.

Data availability

Data generated in this study have been submitted to the NCBI Gene Expression Omnibus (GEO; http://www.ncbi.nlm.nih.gov/geo/) under accession numbers GSE109084 (related to Fig 1) and GSE108680 (related to Fig 6).

Expanded View for this article is available online.

Acknowledgements
We thank Howard Chang and members of the Rana Lab for helpful discussions and advice. We are grateful to Xiayu Stacy Huang and Alexey Eroshkin of The Genomics and Informatics and Data Management core facilities at Sanford Burnham Prebys Medical Discovery Institute for help in data analysis. We thank Steve Head and the staff of the Next Generation Sequencing core facility at The Scripps Research Institute for help with the HT-seq. This work was supported in part by NIH grants to TMR (CA177322, DP1DA039562, AI125103, DA046171).

Author contributions
QZ, T-CC, VSP, and TMR designed experiments. VSP performed initial studies to generate gene expression data in response to TLR activation. QZ and T-CC performed experiments to identify *cis*-regulation and mechanistic studies. YQ analyzed *cis*-regulatory ncRNAs and coding gene expression. SKT analyzed immune mechanisms. JC and KJG analyzed lincRNA and coding genes genetic variation in diseases. AD and TRG analyzed RNA-seq data after TLR ligand stimulation. ZL and JD contributed to TLR stimulation experiments. SG analyzed RNA-seq data and pathways analysis in *ROCKI* overexpression and *MARCKS* KD. C-MT and VN participated in GBS studies. KU participated in analyzing ncRNAs relevance in TB. QZ, T-CC, and TMR wrote the manuscript with input from authors.

Conflict of interest
TMR is a founder of ViRx Pharmaceuticals and a member of its scientific advisory board. The terms of this arrangement have been reviewed and approved by the University of California, San Diego in accordance with its conflict of interest policies.

References

Aderem AA, Albert KA, Keum MM, Wang JK, Greengard P, Cohn ZA (1988) Stimulus-dependent myristoylation of a major substrate for protein kinase C. *Nature* 332: 362 – 364

Atianand MK, Hu W, Satpathy AT, Shen Y, Ricci EP, Alvarez-Dominguez JR, Bhatta A, Schattgen SA, McGowan JD, Blin J, Braun JE, Gandhi P, Moore MJ, Chang HY, Lodish HF, Caffrey DR, Fitzgerald KA (2016) A long noncoding RNA lincRNA-EPS acts as a transcriptional brake to restrain inflammation. *Cell* 165: 1672 – 1685

Bhakat KK, Izumi T, Yang SH, Hazra TK, Mitra S (2003) Role of acetylated human AP-endonuclease (APE1/Ref-1) in regulation of the parathyroid hormone gene. *EMBO J* 22: 6299 – 6309

Bhakat KK, Mantha AK, Mitra S (2009) Transcriptional regulatory functions of mammalian AP-endonuclease (APE1/Ref-1), an essential multifunctional protein. *Antioxid Redox Signal* 11: 621 – 638

Cabili MN, Trapnell C, Goff L, Koziol M, Tazon-Vega B, Regev A, Rinn JL (2011) Integrative annotation of human large intergenic noncoding RNAs reveals global properties and specific subclasses. *Genes Dev* 25: 1915 – 1927

Carpenter S, Aiello D, Atianand MK, Ricci EP, Gandhi P, Hall LL, Byron M, Monks B, Henry-Bezy M, Lawrence JB, O'Neill LA, Moore MJ, Caffrey DR, Fitzgerald KA (2013) A long noncoding RNA mediates both activation and repression of immune response genes. *Science* 341: 789 – 792

Cech TR, Steitz JA (2014) The noncoding RNA revolution-trashing old rules to forge new ones. *Cell* 157: 77 – 94

Chen L, Ge B, Casale FP, Vasquez L, Kwan T, Garrido-Martín D, Watt S, Yan Y, Kundu K, Ecker S, Datta A, Richardson D, Burden F, Mead D, Mann AL, Fernandez JM, Rowlston S, Wilder SP, Farrow S, Shao X *et al* (2016) Genetic drivers of epigenetic and transcriptional variation in human immune cells. *Cell* 167: 1398 – 1414.e1324

Chen YG, Satpathy AT, Chang HY (2017) Gene regulation in the immune system by long noncoding RNAs. *Nat Immunol* 18: 962 – 972

Chu C, Quinn J, Chang HY (2012) Chromatin isolation by RNA purification (ChIRP). *J Vis Exp* https://doi.org/10.3791/3912

Consortium GT, Laboratory DA, Coordinating Center -Analysis Working G, Statistical Methods groups-Analysis Working G, Enhancing Gg, Fund NIHC, Nih/Nci, Nih/Nhgri, Nih/Nimh, Nih/Nida, Biospecimen Collection Source Site N, Biospecimen Collection Source Site R, Biospecimen Core Resource V, Brain Bank Repository-University of Miami Brain Endowment B, Leidos Biomedical-Project M, Study E, Genome Browser Data I, Visualization EBI, Genome Browser Data I, Visualization-Ucsc Genomics Institute UoCSC, Lead a, Laboratory DA, Coordinating C, management NIHp, Biospecimen c, Pathology, e QTLmwg, Battle A, Brown CD, Engelhardt BE, Montgomery SB (2017) Genetic effects on gene expression across human tissues. *Nature* 550: 204 – 213

Deliard S, Zhao J, Xia Q, Grant SF (2013) Generation of high quality chromatin immunoprecipitation DNA template for high-throughput sequencing (ChIP-seq). *J Vis Exp* https://doi.org/10.3791/50286

Engreitz JM, Haines JE, Perez EM, Munson G, Chen J, Kane M, McDonel PE, Guttman M, Lander ES (2016) Local regulation of gene expression by lncRNA promoters, transcription and splicing. *Nature* 539: 452 – 455

Fuchs S, Philippe J, Corvol P, Pinet F (2003) Implication of Ref-1 in the repression of renin gene transcription by intracellular calcium. *J Hypertens* 21: 327 – 335

Gadi D, Wagenknecht-Wiesner A, Holowka D, Baird B (2011) Sequestration of phosphoinositides by mutated MARCKS effector domain inhibits stimulated Ca(2+) mobilization and degranulation in mast cells. *Mol Biol Cell* 22: 4908 – 4917

Gay NJ, Gangloff M (2007) Structure and function of Toll receptors and their ligands. *Annu Rev Biochem* 76: 141 – 165

Giambartolomei C, Vukcevic D, Schadt EE, Franke L, Hingorani AD, Wallace C, Plagnol V (2014) Bayesian test for colocalisation between pairs of genetic association studies using summary statistics. *PLoS Genet* 10: e1004383

Gilbert LA, Larson MH, Morsut L, Liu Z, Brar GA, Torres SE, Stern-Ginossar N, Brandman O, Whitehead EH, Doudna JA, Lim WA, Weissman JS, Qi LS (2013) CRISPR-mediated modular RNA-guided regulation of transcription in eukaryotes. *Cell* 154: 442 – 451

Guil S, Esteller M (2012) Cis-acting noncoding RNAs: friends and foes. *Nat Struct Mol Biol* 19: 1068 – 1075

Harlan DM, Graff JM, Stumpo DJ, Eddy RL Jr, Shows TB, Boyle JM, Blackshear PJ (1991) The human myristoylated alanine-rich C kinase substrate (MARCKS) gene (MACS). Analysis of its gene product, promoter, and chromosomal localization. *J Biol Chem* 266: 14399 – 14405

Hartwig JH, Thelen M, Rosen A, Janmey PA, Nairn AC, Aderem A (1992) Marcks is an actin filament cross-linking protein regulated by protein-kinase-C and calcium calmodulin. *Nature* 356: 618 – 622

Henneke P, Dramsi S, Mancuso G, Chraibi K, Pellegrini E, Theilacker C, Hubner J, Santos-Sierra S, Teti G, Golenbock DT, Poyart C, Trieu-Cuot P (2008) Lipoproteins are critical TLR2 activating toxins in group B streptococcal sepsis. *J Immunol* 180: 6149 – 6158

Hezroni H, Ben-Tov Perry R, Meir Z, Housman G, Lubelsky Y, Ulitsky I (2017) A subset of conserved mammalian long non-coding RNAs are fossils of ancestral protein-coding genes. *Genome Biol* 18: 162

Housman G, Ulitsky I (2016) Methods for distinguishing between protein-coding and long noncoding RNAs and the elusive biological purpose of translation of long noncoding RNAs. *Biochem Biophys Acta* 1859: 31 – 40

Imamura K, Imamachi N, Akizuki G, Kumakura M, Kawaguchi A, Nagata K, Kato A, Kawaguchi Y, Sato H, Yoneda M, Kai C, Yada T, Suzuki Y, Yamada T, Ozawa T, Kaneki K, Inoue T, Kobayashi M, Kodama T, Wada Y *et al* (2014) Long noncoding RNA NEAT1-dependent SFPQ relocation from promoter region to paraspeckle mediates IL8 expression upon immune stimuli. *Mol Cell* 53: 393 – 406

Ingolia NT, Ghaemmaghami S, Newman JRS, Weissman JS (2009) Genome-wide analysis *in vivo* of translation with nucleotide resolution using ribosome profiling. *Science* 324: 218 – 223

Iwasaki A, Medzhitov R (2015) Control of adaptive immunity by the innate immune system. *Nat Immunol* 16: 343 – 353

Joung J, Engreitz JM, Konermann S, Abudayyeh OO, Verdine VK, Aguet F, Gootenberg JS, Sanjana NE, Wright JB, Fulco CP, Tseng YY, Yoon CH, Boehm JS, Lander ES, Zhang F (2017) Genome-scale activation screen identifies a lncRNA locus regulating a gene neighbourhood. *Nature* 548: 343 – 346

Kawai T, Akira S (2010) The role of pattern-recognition receptors in innate immunity: update on Toll-like receptors. *Nat Immunol* 11: 373 – 384

Khalil AM, Guttman M, Huarte M, Garber M, Raj A, Rivea Morales D, Thomas K, Presser A, Bernstein BE, van Oudenaarden A, Regev A, Lander ES, Rinn JL (2009) Many human large intergenic noncoding RNAs associate with chromatin-modifying complexes and affect gene expression. *Proc Natl Acad Sci USA* 106: 11667 – 11672

Kopp F, Mendell JT (2018) Functional classification and experimental dissection of long noncoding RNAs. *Cell* 172: 393 – 407

Lee HM, Yuk JM, Shin DM, Yang CS, Kim KK, Choi DK, Liang ZL, Kim JM, Jeon BH, Kim CD, Lee JH, Jo EK (2009) Apurinic/apyrimidinic endonuclease 1 is a key modulator of keratinocyte inflammatory responses. *J Immunol* 183: 6839 – 6848

Lee SM, Suk K, Lee WH (2015) Myristoylated alanine-rich C kinase substrate (MARCKS) regulates the expression of proinflammatory cytokines in macrophages through activation of p38/JNK MAPK and NF-kappaB. *Cell Immunol* 296: 115 – 121

Lehnardt S, Henneke P, Lien E, Kasper DL, Volpe JJ, Bechmann I, Nitsch R, Weber JR, Golenbock DT, Vartanian T (2006) A mechanism for neurodegeneration induced by group B streptococci through activation of the TLR2/MyD88 pathway in microglia. *J Immunol* 177: 583 – 592

Lemaitre B (2004) The road to toll. *Nat Rev Immunol* 4: 521 – 527

Li Z, Chao TC, Chang KY, Lin N, Patil VS, Shimizu C, Head SR, Burns JC, Rana TM (2014) The long noncoding RNA THRIL regulates TNFalpha expression through its interaction with hnRNPL. *Proc Natl Acad Sci USA* 111: 1002 – 1007

Lin N, Chang K-Y, Li Z, Gates K, Rana Zacharia A, Dang J, Zhang D, Han T, Yang C-S, Cunningham TJ, Head SR, Duester G, Dong PDS, Rana TM (2014) An evolutionarily conserved long noncoding RNA TUNA controls pluripotency and neural lineage commitment. *Mol Cell* 53: 1005 – 1019

Luo S, Lu JY, Liu L, Yin Y, Chen C, Han X, Wu B, Xu R, Liu W, Yan P, Shao W, Lu Z, Li H, Na J, Tang F, Wang J, Zhang YE, Shen X (2016) Divergent lncRNAs regulate gene expression and lineage differentiation in pluripotent cells. *Cell Stem Cell* 18: 637 – 652

Mancek-Keber M, Bencina M, Japelj B, Panter G, Andra J, Brandenburg K, Triantafilou M, Triantafilou K, Jerala R (2012) MARCKS as a negative regulator of lipopolysaccharide signaling. *J Immunol* 188: 3893 – 3902

Maurano MT, Humbert R, Rynes E, Thurman RE, Haugen E, Wang H, Reynolds AP, Sandstrom R, Qu H, Brody J, Shafer A, Neri F, Lee K, Kutyavin T, Stehling-Sun S, Johnson AK, Canfield TK, Giste E, Diegel M, Bates D *et al* (2012) Systematic localization of common disease-associated variation in regulatory DNA. *Science* 337: 1190 – 1195

Mogensen TH (2009) Pathogen recognition and inflammatory signaling in innate immune defenses. *Clin Microbiol Rev* 22: 240 – 273

Mondal T, Rasmussen M, Pandey GK, Isaksson A, Kanduri C (2010) Characterization of the RNA content of chromatin. *Genome Res* 20: 899 – 907

Orom UA, Derrien T, Beringer M, Gumireddy K, Gardini A, Bussotti G, Lai F, Zytnicki M, Notredame C, Huang Q, Guigo R, Shiekhattar R (2010) Long noncoding RNAs with enhancer-like function in human cells. *Cell* 143: 46 – 58

Pacis A, Tailleux L, Morin AM, Lambourne J, MacIsaac JL, Yotova V, Dumaine A, Danckaert A, Luca F, Grenier JC, Hansen KD, Gicquel B, Yu M, Pai A, He C, Tung J, Pastinen T, Kobor MS, Pique-Regi R, Gilad Y *et al* (2015) Bacterial infection remodels the DNA methylation landscape of human dendritic cells. *Genome Res* 25: 1801 – 1811

Quinn JJ, Chang HY (2016) Unique features of long non-coding RNA biogenesis and function. *Nat Rev Genet* 17: 47 – 62

Rapicavoli NA, Qu K, Zhang J, Mikhail M, Laberge RM, Chang HY (2013) A mammalian pseudogene lncRNA at the interface of inflammation and anti-inflammatory therapeutics. *Elife* 2: e00762

Rodriguez Pena MJ, Castillo Bennett JV, Soler OM, Mayorga LS, Michaut MA (2013) MARCKS protein is phosphorylated and regulates calcium mobilization during human acrosomal exocytosis. *PLoS ONE* 8: e64551

Seykora JT, Ravetch JV, Aderem A (1991) Cloning and molecular characterization of the murine macrophage "68-kDa" protein kinase C substrate and its regulation by bacterial lipopolysaccharide. *Proc Natl Acad Sci USA* 88: 2505 – 2509

Sigova AA, Mullen AC, Molinie B, Gupta S, Orlando DA, Guenther MG, Almada AE, Lin C, Sharp PA, Giallourakis CC, Young RA (2013) Divergent transcription of long noncoding RNA/mRNA gene pairs in embryonic stem cells. *Proc Natl Acad Sci USA* 110: 2876 – 2881

Song DH, Lee JO (2012) Sensing of microbial molecular patterns by Toll-like receptors. *Immunol Rev* 250: 216 – 229

Thelen M, Rosen A, Nairn AC, Aderem A (1990) Tumor necrosis factor alpha modifies agonist-dependent responses in human neutrophils by inducing the synthesis and myristoylation of a specific protein kinase C substrate. *Proc Natl Acad Sci USA* 87: 5603 – 5607

Wakefield J (2009) Bayes factors for genome-wide association studies: comparison with P-values. *Genet Epidemiol* 33: 79 – 86

Wang L, Liu X, Lenox RH (2002) Transcriptional regulation of mouse MARCKS promoter in immortalized hippocampal cells. *Biochem Biophys Res Comm* 292: 969 – 979

Wang P, Xue Y, Han Y, Lin L, Wu C, Xu S, Jiang Z, Xu J, Liu Q, Cao X (2014) The STAT3-binding long noncoding RNA lnc-DC controls human dendritic cell differentiation. *Science* 344: 310 – 313

Wang P, Xu J, Wang Y, Cao X (2017) An interferon-independent lncRNA promotes viral replication by modulating cellular metabolism. *Science* 358: 1051 – 1055

